

cy.2



SENSITIVITY OF AIRCRAFT SPINNING MOTION TO DYNAMIC CROSS-COUPLING AND ACCELERATION DERIVATIVES

**R. W. Butler and T. F. Langham
ARO, Inc., a Sverdrup Corporation Company**

**PROPULSION WIND TUNNEL FACILITY
ARNOLD ENGINEERING DEVELOPMENT CENTER
AIR FORCE SYSTEMS COMMAND
ARNOLD AIR FORCE STATION, TENNESSEE 37389**

October 1978

Final Report for Period October 1, 1976 - September 30, 1977

Approved for public release; distribution unlimited.

*Property of U. S. Air Force
AEDC LIBRARY
FSC600-12-C-0009*

Prepared for

**ARNOLD ENGINEERING DEVELOPMENT CENTER/DOTR
ARNOLD AIR FORCE STATION, TENNESSEE 37389**

NOTICES

When U. S. Government drawings, specifications, or other data are used for any purpose other than a definitely related Government procurement operation, the Government thereby incurs no responsibility nor any obligation whatsoever, and the fact that the Government may have formulated, furnished, or in any way supplied the said drawings, specifications, or other data, is not to be regarded by implication or otherwise, or in any manner licensing the holder or any other person or corporation, or conveying any rights or permission to manufacture, use, or sell any patented invention that may in any way be related thereto.

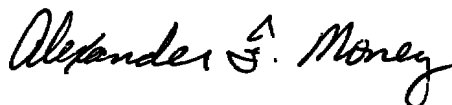
Qualified users may obtain copies of this report from the Defense Documentation Center.

References to named commercial products in this report are not to be considered in any sense as an indorsement of the product by the United States Air Force or the Government.

This report has been reviewed by the Information Office (OI) and is releasable to the National Technical Information Service (NTIS). At NTIS, it will be available to the general public, including foreign nations.

APPROVAL STATEMENT

This report has been reviewed and approved.



ALEXANDER F. MONEY
Project Manager, Research Division
Directorate of Test Engineering

Approved for publication:

FOR THE COMMANDER



ROBERT W. CROSSLEY, Lt Colonel, USAF
Acting Director of Test Engineering
Deputy for Operations

UNCLASSIFIED

REPORT DOCUMENTATION PAGE		READ INSTRUCTIONS BEFORE COMPLETING FORM
1. REPORT NUMBER AEDC-TR-78-12	2. GOVT ACCESSION NO.	3. RECIPIENT'S CATALOG NUMBER
4. TITLE (and Subtitle) SENSITIVITY OF AIRCRAFT SPINNING MOTION TO DYNAMIC CROSS-COUPLING AND ACCEL- ERATION DERIVATIVES		5. TYPE OF REPORT & PERIOD COVERED Final Report, Oct 1, 1976 - Sept 30, 1977
7. AUTHOR(s) R. W. Butler and T. F. Langham, ARO, Inc.		6. PERFORMING ORG. REPORT NUMBER
9. PERFORMING ORGANIZATION NAME AND ADDRESS Arnold Engineering Development Center/DOT Air Force Systems Command Arnold Air Force Station, Tennessee 37389		8. CONTRACT OR GRANT NUMBER(s)
11. CONTROLLING OFFICE NAME AND ADDRESS Arnold Engineering Development Center/DOS Arnold Air Force Station, Tennessee 37389		10. PROGRAM ELEMENT, PROJECT, TASK AREA & WORK UNIT NUMBERS Program Element 65807F
14. MONITORING AGENCY NAME & ADDRESS (if different from Controlling Office)		12. REPORT DATE October 1978
		13. NUMBER OF PAGES 46
		15. SECURITY CLASS. (of this report) UNCLASSIFIED
		15a. DECLASSIFICATION/DOWNGRADING SCHEDULE N/A
16. DISTRIBUTION STATEMENT (of this Report) Approved for public release; distribution unlimited.		
17. DISTRIBUTION STATEMENT (of the abstract entered in Block 20, if different from Report)		
18. SUPPLEMENTARY NOTES Available in DDC		
19. KEY WORDS (Continue on reverse side if necessary and identify by block number) sensitivity F-5 aircraft motion captive tests simulation wind tunnel tests		
20. ABSTRACT (Continue on reverse side if necessary and identify by block number) An investigation was conducted to provide an insight into the importance of dynamic cross-coupling and acceleration derivatives in the spinning motion of fighter aircraft. The basic spinning motion of two aircraft was generated with a six-degree-of-freedom motion simulation program. The dynamic cross-coupling and accel- eration derivatives C_{m_p}, C_{m_r}, C_{l_q}, C_{n_q}, $C_{n_{\dot{\beta}}}$, and $C_{l_{\dot{\beta}}}$ were input		

UNCLASSIFIED

UNCLASSIFIED

20. ABSTRACT (Continued)

into the program both individually and simultaneously to note their effect on the time history of spinning motion. Results of the study indicate that the dynamic derivatives can produce significant effects on the aircraft spinning motion and should be considered when conducting a spin analysis. The study also indicates that the spinning motion sensitivity to the dynamic cross-coupling and acceleration derivatives investigated is configuration dependent.

PREFACE

The work reported herein was conducted by the Arnold Engineering Development Center (AEDC), Air Force Systems Command (AFSC), under Program Element 65807F. The results of this research were obtained by ARO, Inc., AEDC Division (a Sverdrup Corporation Company), operating contractor for the AEDC, AFSC, Arnold Air Force Station, Tennessee, under ARO Project No. P32A-K9A. A. F. Money was the Air Force project manager. Analysis of the data was completed on September 30, 1977, and the manuscript was submitted for publication on January 11, 1978.

CONTENTS

	<u>Page</u>
1.0 INTRODUCTION	5
2.0 BACKGROUND	6
3.0 METHOD OF ANALYSIS	6
4.0 TECHNICAL DATA	
4.1 Aircraft Configurations	8
4.2 Basic Aerodynamic and Inertia Data	8
5.0 RESULTS AND DISCUSSION	
5.1 Baseline Spinning Motion	9
5.2 Dynamic Derivative Variations	9
6.0 CONCLUDING REMARKS	14
REFERENCES	14

ILLUSTRATIONS

Figure

1. Aircraft Body-Axis System	17
2. Three-View Sketch of Attack Aircraft	18
3. Three-View Sketch of Fighter Bomber Aircraft	19
4. Aircraft Mass Distribution	20
5. Attack Aircraft Baseline Spinning Motion	21
6. Fighter Bomber Aircraft Baseline Spinning Motion	22
7. Spin Sensitivity to C_{m_p} Variation	23
8. Spin Sensitivity to C_{m_r} Variation	25
9. Spin Sensitivity to C_{l_q} Variation	27
10. Spin Sensitivity to C_{n_q} Variation	29
11. Spin Sensitivity to $C_{n_{\dot{\beta}}}$ Variation	31
12. Spin Sensitivity to $C_{l_{\dot{\beta}}}$ Variation	33
13. Simultaneous Derivative Variation	35

TABLES

1. Aircraft Physical and Mass Characteristics	37
2. Cross-Coupling and Acceleration Derivatives for Baseline Spin (Body Axis)	37
3. Dynamic Derivative Values for Individual Variations (Body Axis)	38

4. Dynamic Derivatives Used in Simultaneous Variations (Body Axis)	38
---	----

APPENDIXES

A. AERODYNAMIC MATHEMATICAL MODELS	39
B. ROTATIONAL BALANCE DATA IMPLEMENTATION	42
NOMENCLATURE	44

1.0 INTRODUCTION

The simulation of aircraft motion through analytical techniques is becoming a very important tool in the development, testing, and operational phases of modern fighter aircraft programs. A pilot in the loop fixed-base simulators, which in the past have been used primarily for pilot training and proficiency checks, are now being applied to the development and testing phases of new fighter aircraft. An example of this is the NASA differentially maneuvering simulator which has recently been used to study the effectiveness of an automatic control system on an advanced fighter aircraft at high angles of attack (Ref. 1). By using the simulator, a more economical and safer development and evaluation program was conducted than was possible through flight testing.

In the low angle-of-attack unstalled flight regime, the confidence level in motion simulation is high. As the aircraft angle of attack increases to the stall/spin flight regime, the confidence level diminishes correspondingly. This degradation in confidence, resulting from poor "before-the-fact" simulation, is not caused by an inadequacy in the aircraft equations of motion in stall/spin flight but results from improper or inadequate definition of the aircraft aerodynamics in this regime.

New experimental test apparatus in the form of dynamic balances (Ref. 2) and rotational-balance hardware at NASA Langley and Ames are being developed to better define aircraft aerodynamics in stalled and spinning flight. The rotational balance apparatus measures the aerodynamics of an aircraft under steady rotating conditions. This accounts for the nonlinear effect of rotation rate. Preliminary analysis indicates these data are necessary for before-the-fact simulation of an aircraft spinning motion. Little work has been done to define what dynamic oscillatory components should accompany these rotational-balance data in defining data matrices for spinning flight. Generally, the oscillatory direct and cross-damping derivatives are included in spin simulation because of their proven importance in the nonspinning regime. The importance of dynamic cross-coupling and acceleration derivatives in spinning flight is not clearly defined.

The Arnold Engineering Development Center (AEDC) is presently conducting research to define what aerodynamic parameters are necessary for achieving good before-the-fact aircraft motion simulation in the stall/spin flight regime. It is necessary to define these parameters such that future experimental test apparatus may be designed for their measurements.

The subject analysis defines the importance of aircraft cross-coupling and acceleration damping derivatives in the analytical simulation of aircraft spinning motion.

Derivatives investigated in the analysis are C_{m_p} , C_{m_r} , C_{l_q} , C_{n_q} , $C_{n_{\dot{\delta}}}$, and $C_{l_{\dot{\delta}}}$. Two types of aircraft are utilized in the analysis. Changes in one of the predominate spin modes of each aircraft are investigated with both individual and simultaneous variations of cross-coupling and acceleration derivatives. Time histories of the aircraft spinning motion are provided using a six-degree-of-freedom (6-DOF) nonlinear computer program. The analysis addresses only the developed spinning mode of flight; attempts to analyze the incipient or recovery phases of the spin are not included.

2.0 BACKGROUND

Prior to the 1960's, aircraft dynamic cross-coupling and acceleration derivatives were generally considered insignificant in fighter aircraft motion simulation and dynamic stability analysis. These assumptions were good, primarily because aircraft of that era were operating at moderate angles of attack where both cross-coupling and acceleration derivatives possessed small values. In the mid 1960's, it became necessary for these same aircraft to extend their operating envelopes to high angles of attack under combat conditions. As a result of this high-risk operating environment, aircraft were pushed beyond stalled and spinning flight. Attempts to analytically simulate the poststall gyration and spinning flight experienced by the aircraft were generally unsuccessful. When a successful correlation was achieved, it was normally an after-the-fact correlation resulting from many attempts of parameter variations to achieve a suitable combination of aerodynamics. It became apparant that a better representation of the aerodynamics of an aircraft would be necessary for achieving a before-the-fact analytical simulation of aircraft stalled and spinning motion.

An attempt to isolate some of the important aerodynamic parameters in aircraft spinning flight was undertaken by Bihrlé in 1970 (Ref. 3). Dynamic cross and acceleration derivatives were evaluated against spin sensitivity in the analysis. Results indicated the spinning motion to be insensitive to the acceleration derivatives and often sensitive to cross derivatives. Since Bihrlé's work, it has been shown experimentally by NASA (Ref. 4) and Orlik-Ruckemann of the NAE in Canada (Ref. 5) that the magnitude of the acceleration and cross derivatives of aircraft at high angles of attack is much greater than Bihrlé had assumed. Also, the sign of these derivatives often changes at the higher angles. In addition, Ref. 5 shows the aircraft cross-coupling derivatives to have values equal in magnitude to direct derivatives.

3.0 METHOD OF ANALYSIS

The analytical tool used in this dynamic sensitivity analysis was a 6-DOF nonlinear computer program. The program was originally formulated by North American Rockwell

(Ref. 6) using a fourth-order Runge-Kutta integration algorithm with a fixed integration size. The program input and aerodynamic modules have since been modified for adaptation to this study. The program was modified to run interactively with a graphics terminal to expedite the analysis. The 6-DOF equations of motion describing the aircraft motion are rigid-body equations referenced to a body-fixed axis system shown in Fig. 1. The basic equations are as follows:

Forces

$$\begin{aligned}\dot{u} &= rv - qw - q \sin \theta + \frac{F_X}{m} + \frac{T_X}{m} \\ \dot{v} &= pw - ru + q \cos \theta \sin \phi + \frac{F_Y}{m} \\ \dot{w} &= qu - pv + q \cos \theta \cos \phi + \frac{F_Z}{m} + \frac{T_Z}{m}\end{aligned}$$

Moments

$$\begin{aligned}\dot{p} &= \frac{I_Y - I_Z}{I_X} qr + \frac{I_{XZ}}{I_X} (\dot{r} + pq) + \frac{M_X}{I_X} \\ \dot{q} &= \frac{I_Z - I_X}{I_Y} pr + \frac{I_{XZ}}{I_Y} (r^2 - p^2) + \frac{M_Y}{I_Y} + \frac{M_{YT}}{I_Y} + \frac{M_{YG}}{I_Y} \\ \dot{r} &= \frac{I_X - I_Y}{I_Z} pq + \frac{I_{XZ}}{I_Z} (\dot{p} - qr) + \frac{M_Z}{I_Z} + \frac{M_{ZG}}{I_Z}\end{aligned}$$

The external forces and moments (F_X , F_Y , F_Z , M_X , M_Y , M_Z) in the equations are comprised of aerodynamic coefficients representative of the aircraft. Formulation of the aerodynamic mathematical models used in representing each of these aircraft is presented in Appendix A. It should be noted that the aerodynamic data matrix for the attack aircraft consists of static and dynamic oscillatory data, whereas the data matrices for the fighter bomber have static, dynamic oscillatory, and rotational-balance data. All aerodynamic data used in the mathematical model of Appendix A are experimental and are discussed in more detail in Section 4.2. The method used in implementing the rotational balance data for the fighter bomber is outlined in Appendix B.

Additional basic equations used in the subject analysis are given below:

$$\begin{aligned}\alpha &= \tan^{-1} \frac{u}{w} & \beta &= \sin^{-1} \left(\frac{v}{V_\infty} \right) \\ V_\infty &= \sqrt{u^2 + v^2 + w^2} & \Omega &= \sqrt{p^2 + q^2 + r^2} \\ \Omega_{ss} &= \frac{up + vq + wr}{|V_\infty|}\end{aligned}$$

An explanation of the steady-state rotational rate vector (Ω_{ss}) is given in Appendix B. Time histories of the aircraft spinning motion were generated using this 6-DOF computer program. Angular motion changes about the aircraft center of gravity and changes in the center-of-gravity path with either individual or simultaneous variations of the derivatives were used to ascertain the significance of the derivatives in spinning motion simulation.

4.0 TECHNICAL DATA

4.1 AIRCRAFT CONFIGURATIONS

Two aircraft configurations were chosen for the spinning motion sensitivity study. The selection of these aircraft was influenced by previous dynamic sensitivity studies (Ref. 8) conducted at AEDC using the same configurations. Also, it was felt that aircraft should be used for which a general knowledge of the spin characteristics exists. Aircraft similar to each of the selected configurations have been involved in stall/spin test programs (Refs. 9 and 10) identifying their basic spin characteristics.

The attack-type configuration, a single engine swept wing aircraft, is shown in Fig. 2 with overall basic dimensions. The fighter bomber type, a twin engine and swept wing aircraft, is shown in Fig. 3, along with overall basic dimensions.

4.2 BASIC AERODYNAMIC AND INERTIA DATA

The aerodynamic data matrices used in modeling the attack aircraft were obtained from the Navy in an unpublished form. The fighter bomber data matrices were formulated from data presented in Refs. 11 and 12. The basic matrices are a combination of static and dynamic oscillatory aerodynamic data. Data are input to the matrices in table look-up form as functions of the variables shown in the equations of Appendix A. The fighter bomber data matrix also includes rotational balance data, previously used in Ref. 7, as an increment to the basic aerodynamics. The attack aircraft data matrix does not include rotational data. Neither of the data matrices has been corrected for Reynolds number, flexibility, or inertia effects experienced in full-scale flight.

Mass and inertia characteristics of the aircraft configurations are presented in Table 1. Although the magnitudes of the mass and inertia of the two aircraft are considerably different, their mass distributions along the reference axis are similar. Figure 4 presents mass distributions of several modern fighter aircraft in the military inventory. With the exception of the F-5, all of these aircraft have similar mass distributions along the reference axis similar to the aircraft used in the project investigation.

5.0 RESULTS AND DISCUSSION

5.1 BASELINE SPINNING MOTION

The approach used for conducting the dynamic sensitivity study was to first establish an equilibrium baseline spinning motion with which other spinning motions could be compared as derivative variations were made. The baseline spins used for the aircraft are shown in Figs. 5 and 6.

The simulated spinning motion of the attack aircraft, Fig. 5, is classified as a steep smooth spin. The motion was initiated from trimmed 1-g flight with control inputs of stick back ($\delta_E = -25$ deg), ailerons neutral ($\delta_A = 0$ deg), and rudder with ($\delta_R = -25$). The spin was entered at an altitude of 21,600 ft. Engine thrust remained constant throughout the spin at 6,400 lb.

The simulated spinning motion of the fighter bomber aircraft, Fig. 6, is classified as flat and compares closely with flat spins experienced in flight tests (Ref. 10). The motion was initiated by inputting conditions (angle of attack, sideslip, rotational rates, etc.) at time zero equal to the equilibrium flat spin parameters of flight data in Ref. 10. By initiating the spin in this manner, prospin controls were not required for entering or maintaining the spin. Lateral directional control surfaces remained in the zero position and the elevator remained at 3 deg ($\delta_L = 3$ deg). The spin was initiated at an altitude of 12,500 ft. Engine thrust was maintained near zero throughout the maneuver.

The dynamic derivatives (C_{m_p} , C_{m_r} , C_{l_q} , C_{n_q} , $C_{n_{\dot{\beta}}}$, and $C_{l_{\dot{\beta}}}$) investigated in the dynamic sensitivity study were each given nominal values in the above baseline spins. The values used were selected from experimental data (Refs. 4 and 5) obtained on airplane-like configurations and are presented in Table 2. The data presented are for angle of attack of approximately 37 deg which corresponds closely to equilibrium spin angle of attack of the attack aircraft. The equilibrium angle of attack of the baseline spin for the fighter bomber aircraft is near 75 deg. Because no experimental data exist for cross-coupling derivatives in this angle-of-attack range, it was decided to use the 37-deg data of Table 2 for the baseline spins for both types of aircraft.

5.2 DYNAMIC DERIVATIVE VARIATIONS

The dynamic derivatives under investigation were input to the baseline spinning maneuvers as constant values at a time when the aircraft spinning motion had reached equilibrium. For the attack-type aircraft, the spin equilibrium was defined to occur at 20

sec into the maneuver, the corresponding time for the fighter bomber type was defined to be 10 sec. In most cases, the derivatives were input individually at these times and remained constant throughout the remaining motion. This allowed the derivative to be isolated in a manner such that its importance in the aircraft spinning motion could be readily evaluated. For a limited number of cases, several of the derivatives were input simultaneously at the above times to provide a more realistic picture of what is occurring in flight.

Experimental data of Refs. 4 and 5 provided a guideline for selecting the maximum and minimum values of the derivatives to be input in the baseline maneuvers. The values selected for each derivative are presented in Table 3. It should be noted that the range of experimental values used in Table 3 was not obtained in a spinning flight environment with associated higher angles of attack (above 40 deg) and the presence of curvilinear flow. Also, the cross-coupling derivative data obtained from Ref. 5 were measured on a cone-wing body, not an actual airplane configuration.

C_{m_p} Derivative

Little is known concerning the magnitude of the cross-coupling derivative C_{m_p} . The experimental work performed by Orlik-Ruckemann presented in Ref. 5 addresses only the cross-coupling derivatives associated with pitching and yawing of the aircraft and does not include C_{m_r} resulting from a rolling motion. Because these works (Ref. 5) represent the only known published literature of measured aircraft cross-coupling derivatives, the relative magnitude of C_{m_p} continues to remain in question. Therefore, in the present sensitivity study it was elected to use C_{m_p} maximum and minimum values identical to those selected from Ref. 5 for the derivative C_{m_r} , -2 to 2 per radian.

The time histories for the C_{m_p} variations compared to the baseline spinning motion in which C_{m_p} possessed a nominal value (Table 2) of zero is presented in Fig. 7. For both aircraft, the negative C_{m_p} coupled with a large negative roll rate (p) produces a driving pitching moment resulting in large longitudinal motion changes with accompanying smaller lateral/directional changes. For the fighter bomber aircraft, the increased oscillations in the longitudinal plane of motion eventually result in the aircraft pitching out of its equilibrium flat spin and entering a form of poststall gyration at the time of approximately 37 sec. Note that in Fig. 7 the mean value of the roll and yaw rates (p and r) are large compared to the pitch rate (q), which is characteristic of a spinning aircraft. When the large p lateral rate is coupled to even a small cross-coupling derivative such as C_{m_p} , the resulting aerodynamic pitching moment can have a significant effect on the aircraft spinning motion.

C_{m_r} Derivative

The second cross-coupling derivative directly affecting the aircraft longitudinal motion is the C_{m_r} derivative. As in the case of the C_{m_p} derivative, the pitching moment resulting from C_{m_r} may be caused by the high yaw rates r associated with spinning motion. Time histories generated with C_{m_r} values of -2 and 2 per radian are shown along with the standard baseline motion in Fig. 8. For the attack aircraft, the motion trends resulting from the C_{m_r} variation are very similar to these for the C_{m_p} variation in Fig. 7.

These similar trends are expected since the ranges of both derivatives are identical and the p and r rates are of the same sign and close in magnitude.

The trends for the fighter bomber spinning motion shown in Figs. 7 and 8 would be expected to be similar with the same derivative variations, but they obviously disagree. The fighter bomber baseline motion is insensitive to the C_{m_r} derivative variation. This insensitivity is a result of the method by which the motion simulation was generated. As pointed out in Appendix A, the fighter bomber aerodynamic data matrix incorporates rotational balance data in the manner described in Appendix B and Ref. 7. To incorporate the rotational data, the total p , q , and r rates were divided into oscillatory and steady-state components. The oscillatory and steady-state components are in turn applied to their corresponding derivatives in the equations of motion. Since the baseline spin for the fighter bomber is flat ($\alpha \approx 75$ deg), the steady-state component of the yaw rate is approximately equal to r (see Appendix B). The oscillatory component of r is in turn near zero, meaning that the resulting pitching-moment contribution from C_{m_r} is near zero, thereby resulting in the insensitivity of the motion to C_{m_r} .

When using rotational balance data (as in Appendix B) for spin simulation, all dynamic oscillatory derivatives caused by yaw rates become increasingly insignificant as angle of attack increases. For conventional spin simulation (no rotational data), the C_{m_r} derivative is significant because of high yaw rates experienced in the spin.

C_{l_q} Derivative

The rolling moment of an aircraft resulting from pitching in the longitudinal plane is described by the cross-coupling derivative C_{l_q} . Time histories of the aircraft spinning motion with variations of this derivative are given in Fig. 9. Although the magnitude of q in the baseline spin is small for the attack aircraft, the C_{l_q} and q combination produces significant effects on the aircraft spinning motion. The negative C_{l_q} actually forces the aircraft out of the spin indicating the aircraft motion is very sensitive to this derivative when considering the magnitude of the q rate. This conclusion is further

verified when viewing the results for the fighter bomber aircraft. Here, the baseline q rate is oscillatory and of larger magnitude than observed in the attack aircraft data. The result is a disruption of the fighter bomber spin almost immediately after the derivative is injected ($t = 10$ sec) to the baseline motion. The data shown in Fig. 9 document that the $C_{\dot{q}_q}$ derivative is the most important of the cross-coupling derivatives in the aircraft spinning motion investigated.

C_{n_q} Derivative

The second cross-coupling derivative resulting from the pitching moment of an aircraft is the yawing moment caused by pitch rate C_{n_q} . The motion sensitivity to the C_{n_q} derivative is presented in Fig. 10 for the two aircraft. It should be noted that the maximum C_{n_q} value of 2 per radian corresponds to the nominal value used in the baseline maneuver; therefore, the two maneuvers are identical. This results from the fact that the angle of attack at which the nominal values of Table 2 were selected is the same angle at which C_{n_q} experiences its maximum value. The minimum value of C_{n_q} (-2 per radian) has a small effect on the motion of both aircraft when compared to the baseline. The primary motion difference is a small increase in the spin rates of both aircraft as seen in the r values. The small changes in frequency of the motion for the fighter bomber are considered to be insignificant. The C_{n_q} derivative appears to be the least significant of all the cross-coupling derivatives in the aircraft spinning motion investigated.

$C_{\dot{q}_\beta}$, C_{n_β} Derivative

In addition to the cross-coupling derivatives, the lateral/directional acceleration derivatives $C_{\dot{q}_\beta}$ and C_{n_β} have also been examined. Recent work presented in Ref. 4 indicates that these derivatives at high angles of attack (angles in the spin regime) may acquire values equal in magnitude to the lateral/directional rate derivatives. The significance of the acceleration derivatives of this magnitude on aircraft spinning motion is shown in Figs. 11 and 12 for C_{n_β} and $C_{\dot{q}_\beta}$, respectively. The values for the derivatives are representative of those obtained experimentally in Ref. 4. The spinning motion for the attack-type aircraft shows significant effects caused by the β variations. The smooth baseline spin becomes oscillatory with the input of the negative C_{n_β} . Likewise, as shown in Fig. 12, the effect of the positive $C_{\dot{q}_\beta}$ causes the aircraft to pitch out of the spin.

In both Figs. 11 and 12 the acceleration derivatives are seen to have a small influence on the motion of the fighter bomber aircraft. Small changes in frequency are noted but the overall nature of the spin remains the same. It should be noted that the

manner in which the rotational aerodynamic data are included in the fighter bomber simulation should not affect the influence of the β derivatives as was the case for the aforementioned C_{m_r} derivative. The acceleration derivative variation indicates (1) the acceleration derivatives can be important in aircraft spin simulation for particular aircraft and, (2) the acceleration derivatives are configuration dependent, and general statements as to their importance may be misleading.

Simultaneous Variations

The major portion of the subject sensitivity study was conducted using individual dynamic derivative changes with all remaining derivatives held constant. This method, in effect, isolates the derivative being investigated such that motion changes with different derivative values can be ascertained. In actual flight, it is impossible to isolate a single derivative in this manner; the magnitudes of all derivatives normally vary simultaneously as the derivative in question is changed. An attempt to more accurately simulate this simultaneous variation is accomplished by first selecting two sets of dynamic data as a function of the independent aerodynamic variable angle of attack. These data are presented in Table 4 for angles of attack of 17 and 26 deg. The angles and corresponding derivatives selected are those from Ref. 5 for C_{l_q} maximum and minimum values of 2 and -2 per radian. The data in Table 4 are in turn input into the aircraft spinning motion together, rather than individually. The time at which the data are input remains the same as in the individual cases.

Time histories presented in Fig. 13 reflect the effect of simultaneous derivative changes on the aircraft maneuvers. Both aircraft experience significant changes in their spinning motion with input of the derivatives. For the attack aircraft, the motion trends are similar to those in Fig. 9 where C_{l_q} was varied individually. In this case, the aircraft motion is predominated by the C_{l_q} derivative even though the other derivatives also changed. For the fighter bomber aircraft, the simultaneous variations caused the aircraft to pitch out of the spin and enter a recovery dive. These motions are representative of those in Fig. 9 when C_{l_q} is -2 per radian but not for the 2 per radian data. Undoubtedly, the smaller derivatives (Table 4) predominated over the C_{l_q} value of 2 per radian in the fighter bomber motion. It is evident from the results of the fighter bomber that the smaller derivatives can have a significant effect on the aircraft motion when acting together. Also, conclusions based on individual derivative variations can be significantly different, depending on the values of the baseline derivatives.

This study has shown the need for dynamic cross-coupling and acceleration derivatives in simulation of aircraft spinning motion when the derivative magnitudes reach those given in Table 3. The final determination of the importance of these derivatives will surface when

their true magnitudes are documented experimentally for an aircraft configuration in a realistic flight regime. If, under these conditions, they possess values approaching those in Table 3, then aerodynamicists should consider including them in spinning motion simulation. The design of future dynamic test apparatus should include the capability of measuring these derivatives such that their true magnitudes can be documented for an aircraft configuration at high angles of attack.

6.0 CONCLUDING REMARKS

As a result of this analysis for spinning aircraft, the following observations and conclusions are offered based on the assumption that the derivatives investigated can acquire values of the magnitude given in Table 3.

1. Because of large r and q rotational rates associated with spinning flight, the pitching moments generated by cross-coupling derivatives C_{m_r} and C_{m_p} may be equal or greater than those generated by the primary derivative C_{m_q} and q rate combination.
2. All cross-coupling and acceleration derivatives C_{m_p} , C_{m_r} , C_{l_q} , C_{n_q} , $C_{n\dot{\beta}}$, and $C_{l\dot{\beta}}$ can produce significant effects on the aircraft spinning motion.
3. Spinning motion sensitivity to the dynamic cross-coupling and acceleration derivatives is configuration dependent.
4. The sensitivity of an aircraft's spinning motion to an individual dynamic derivative variation may vary as a function of the baseline derivatives used in the investigation.
5. The final determination of the importance of the cross-coupling and acceleration derivatives will remain in question until their magnitudes are experimentally measured for an aircraft configuration in a realistic flight regime; experimental test apparatus should be developed for ascertaining these magnitudes.

REFERENCES

1. Gilbert, W. P., Nguyen, L. T., and Van Gunst, R. W. "Simulator Study of the Effectiveness of an Automatic Control System Designed to Improve the High Angle-of-Attack Characteristics of a Fighter Airplane." NASA TN D-8176, May 1976.

2. Hanff, E. S. and Orlik-Ruckermann, K. J. "A Wind Tunnel Test and Calibration Techniques for the Measurement of Damping and Dynamic Cross Derivatives Due to Pitching and Yawing." AIAA Paper No. 77-80, January 1977.
3. Bihrlé, W., Jr. "The Influence of the Static and Dynamic Aerodynamic Characteristics on the Spinning Motion of Aircraft." AIAA Paper 70-946, August 1970.
4. Coc, P. L., Jr., Graham, A. B., and Chambers, J. R. "Summary of Information on Low-Speed Lateral-Directional Derivatives Due to Rate of Change of Sideslip $\dot{\beta}$." NASA TN D-7972, September 1975.
5. Orlik-Ruckermann, K. J. "On Aerodynamic Coupling Between Lateral and Longitudinal Degrees of Freedom." AIAA Paper No. 77-4, January 1977.
6. North American Rockwell. Digital Simulation User's Manual, NR70H-232-2, June 1970.
7. Williams, D. H. "The Use of Rotation-Balance Aerodynamic Data in Theoretical Spin Studies." The George Washington University, School of Engineering, Thesis, August 1976.
8. Butler, R. W. "Aircraft Motion Sensitivity to Cross and Cross-Coupling Damping Derivatives." AEDC-TR-76-138 (ADA032654), November 1976.
9. Smith, D. D., LCDR., Curtis, E. R. Lt., and McNamara, W. G. "Model A-7A/B Airplane Spin Evaluation: Final Report." NATA FT-72R-71 (AD891289L), September 1971.
10. Rutan, E. L., McElory, C. E., and Gentry, J. R. "Stall/Near Stall Investigation of the F-4E Aircraft." AFFTC, FTC-TR-70-20, August 1970.
11. Anglin, Ernie L. "Static Force Tests of a Model of a Twin-Jet Fighter Airplane for Angles of Attack from -10 Degrees to 110 Degrees and Sideslip Angles from -40 Degrees to 40 Degrees." NASA TN D-6425, August 1971.
12. Grafton, Sue B. and Libbey, Charles E. "Dynamic Stability Derivatives of a Twin-Jet Fighter Model for Angles of Attack from -10 Degrees to 110 Degrees." NASA TN D-6091, 1971.

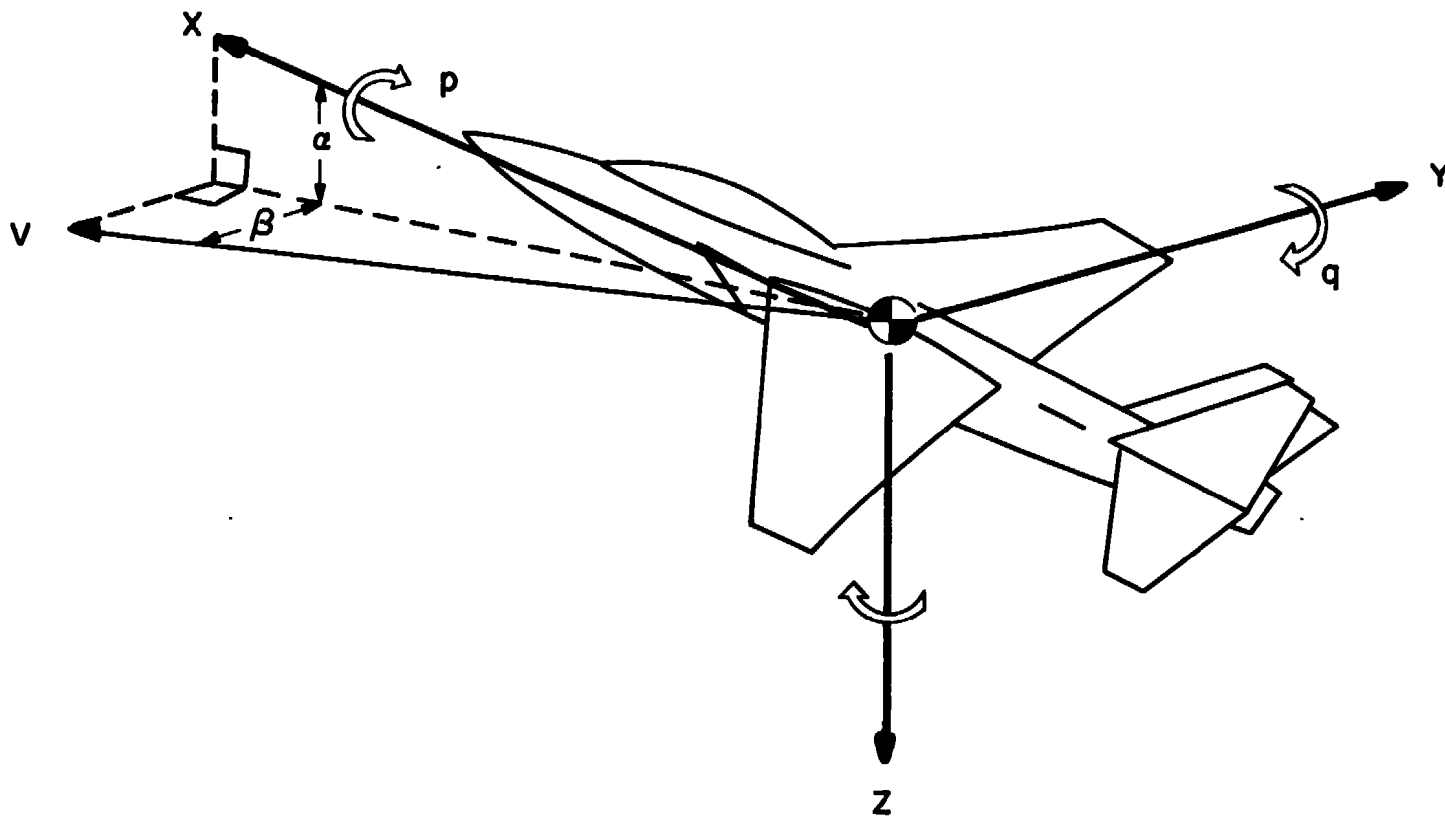
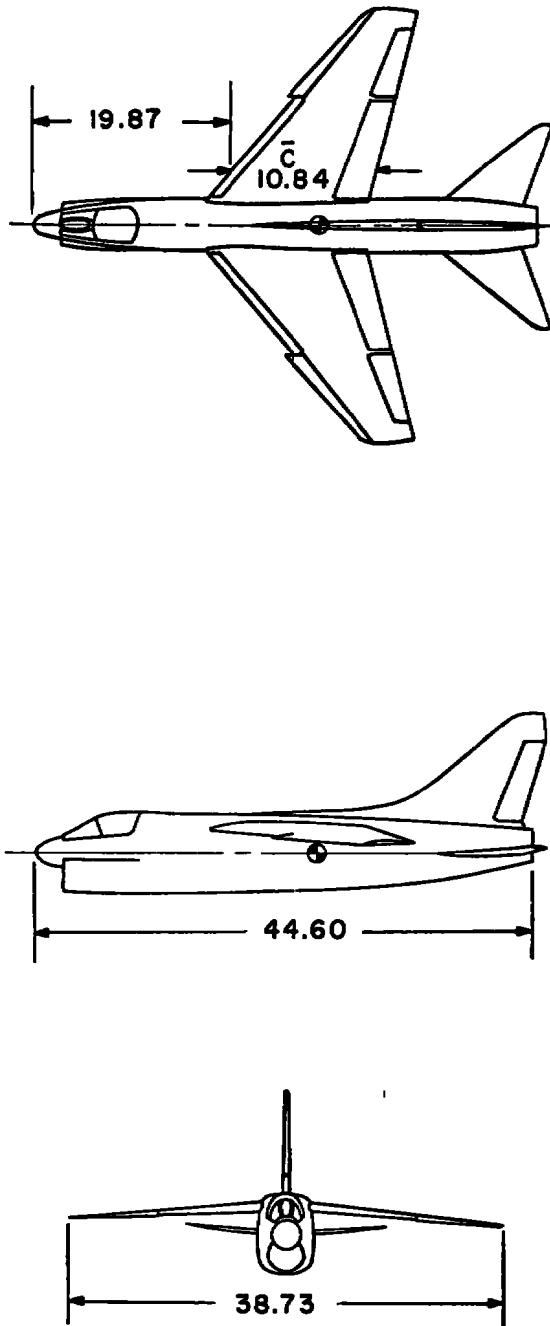
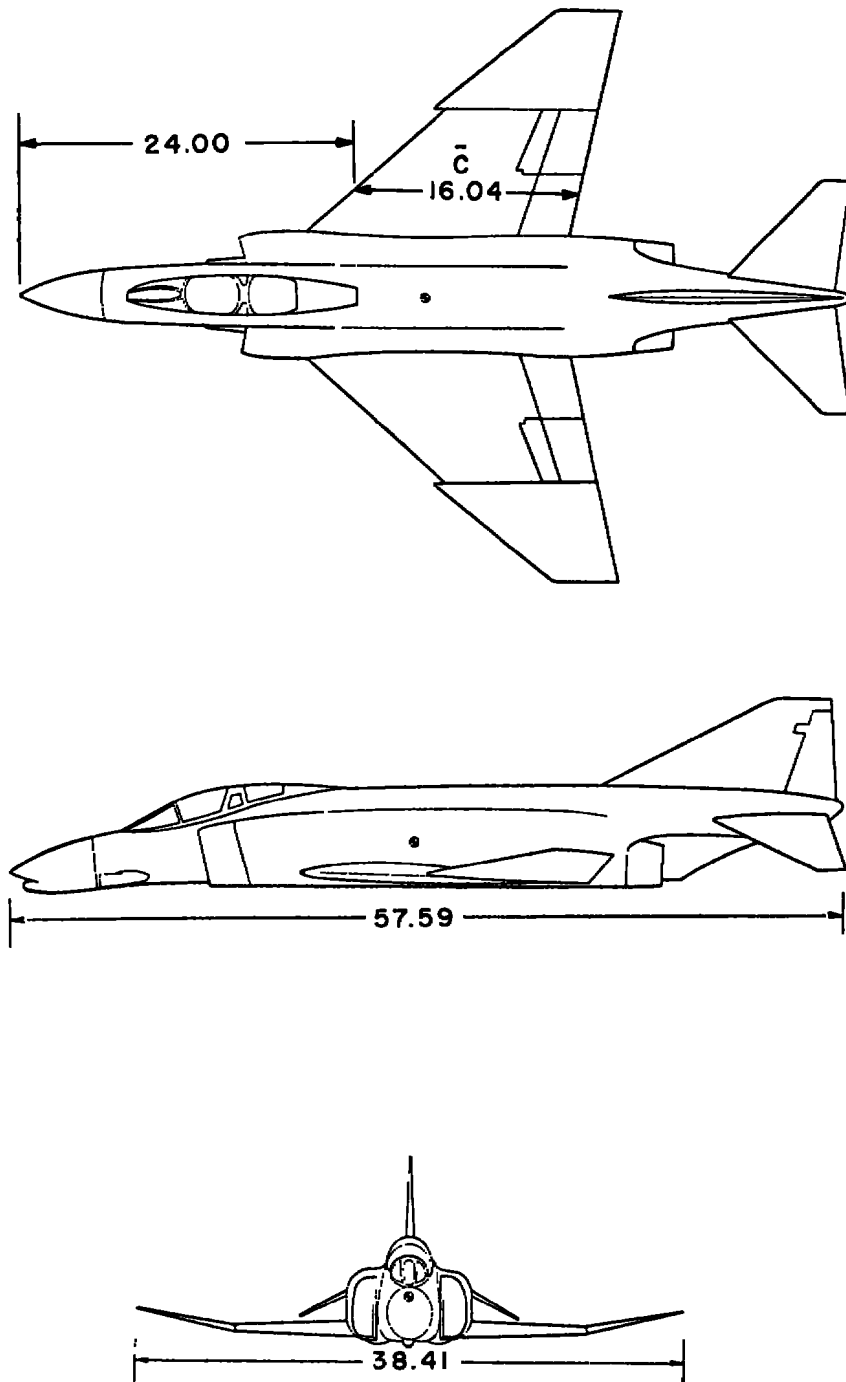


Figure 1. Aircraft body-axis system.



DIMENSIONS IN FEET

Figure 2. Three-view sketch of attack aircraft.



DIMENSIONS IN FEET

Figure 3. Three-view sketch of fighter bomber aircraft.

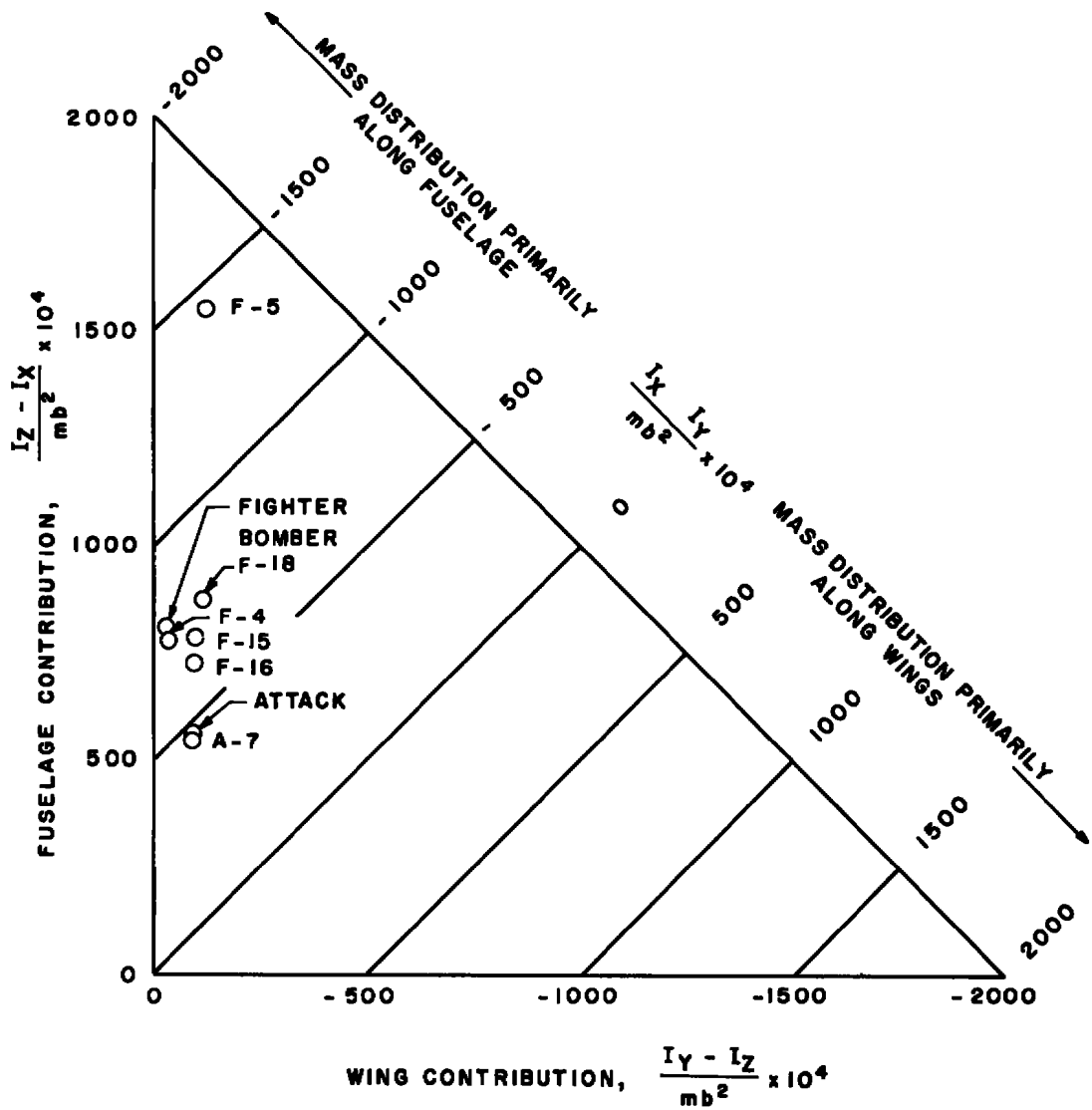


Figure 4. Aircraft mass distribution.

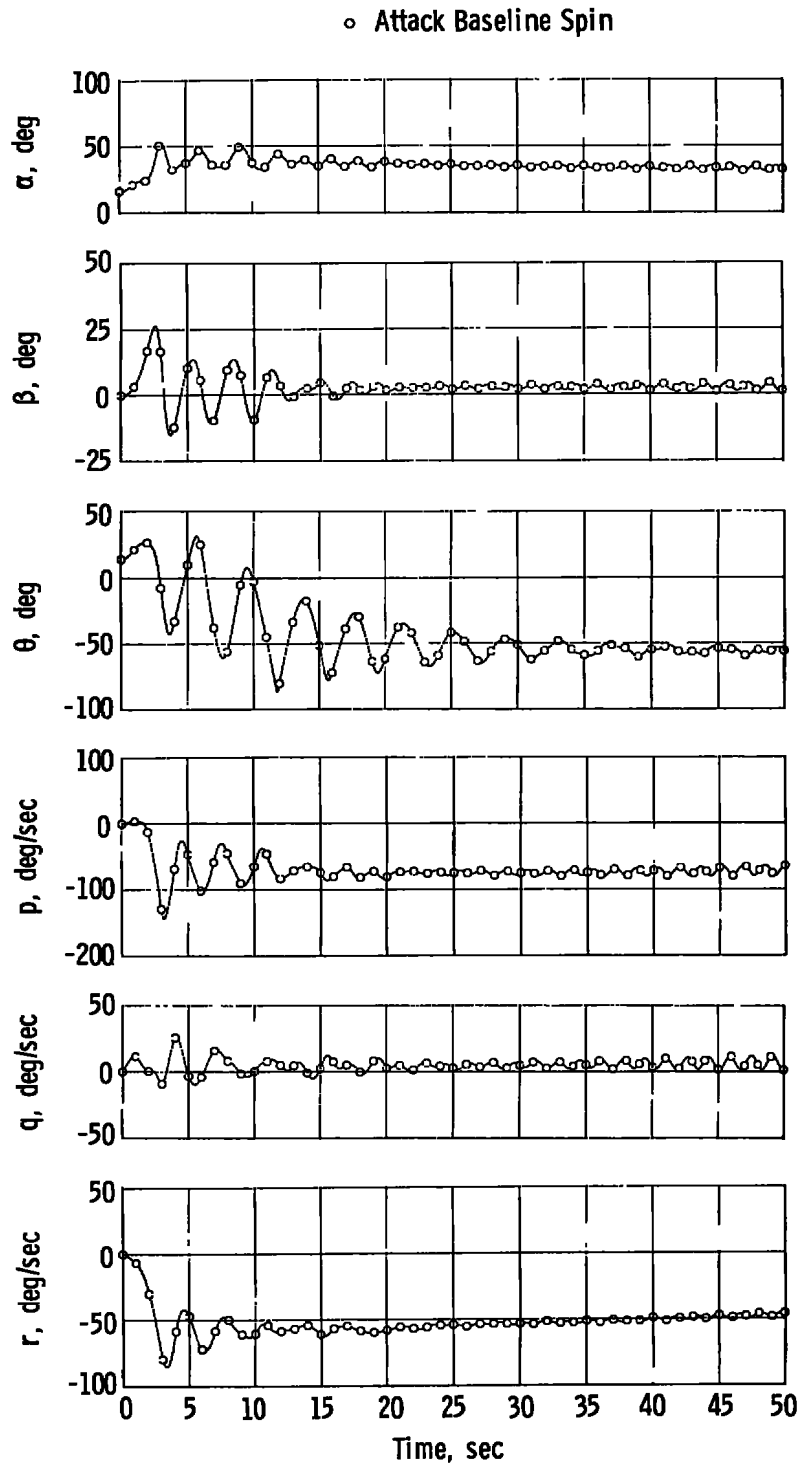


Figure 5. Attack aircraft baseline spinning motion.

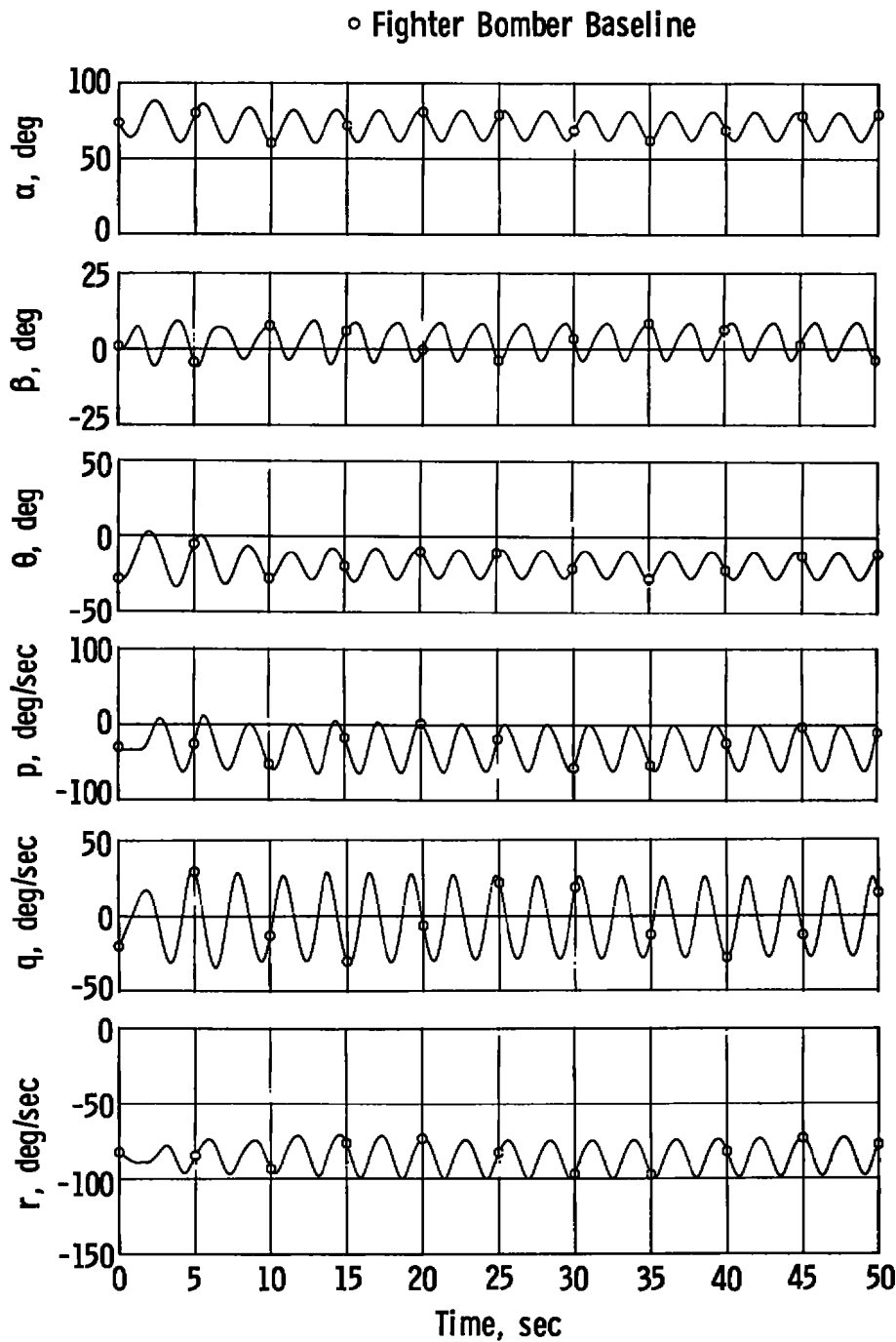
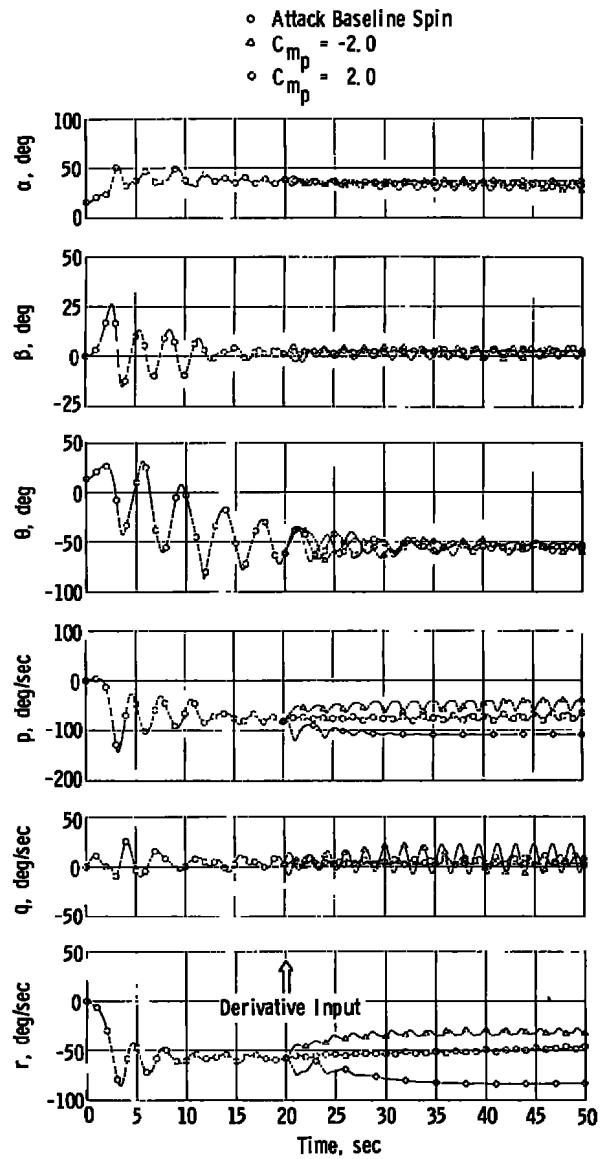
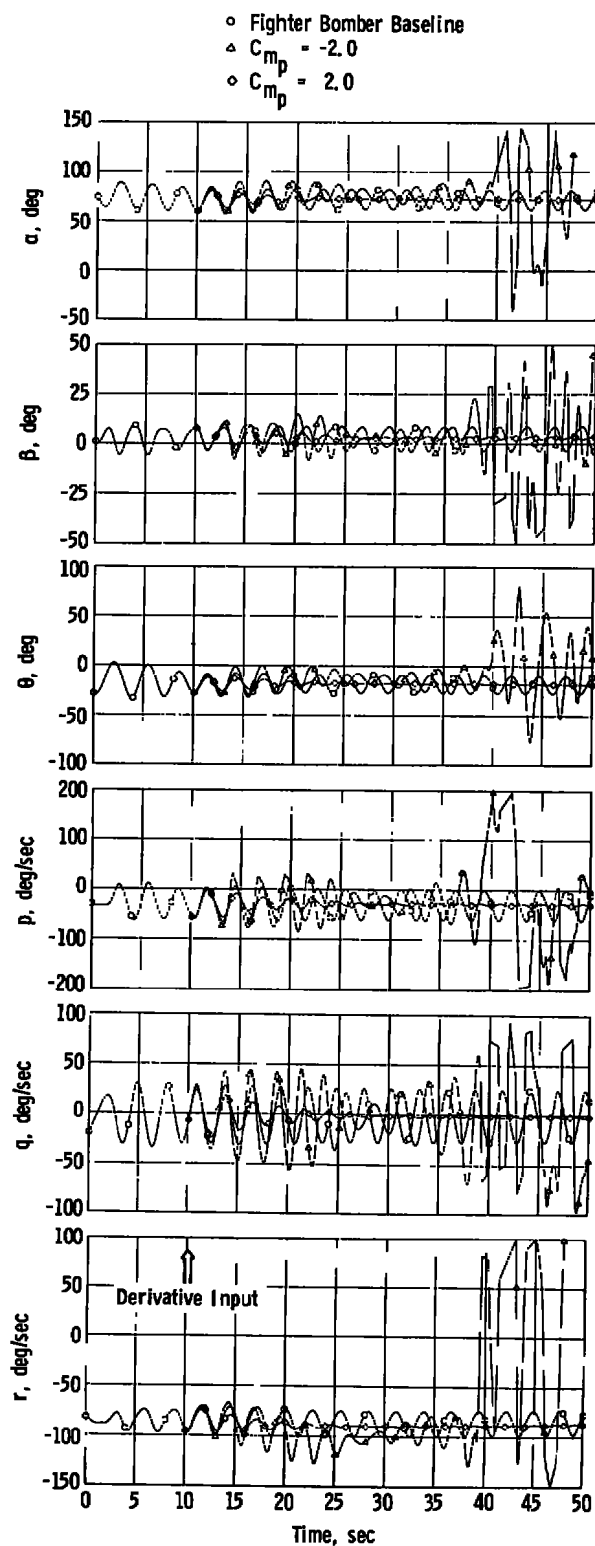


Figure 6. Fighter bomber aircraft baseline spinning motion.

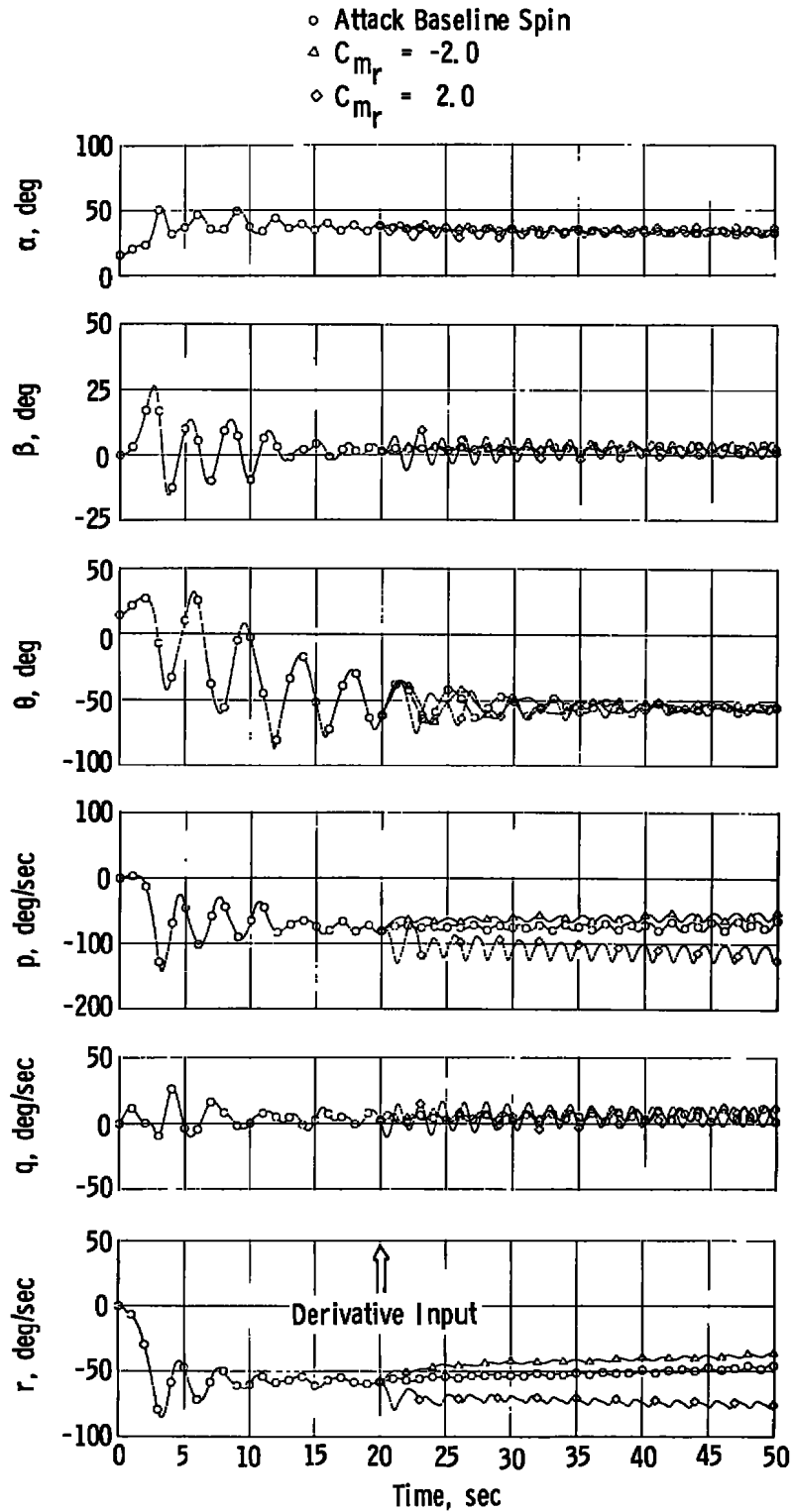


a. Attack-type aircraft

Figure 7. Spin sensitivity to C_{m_p} variation.

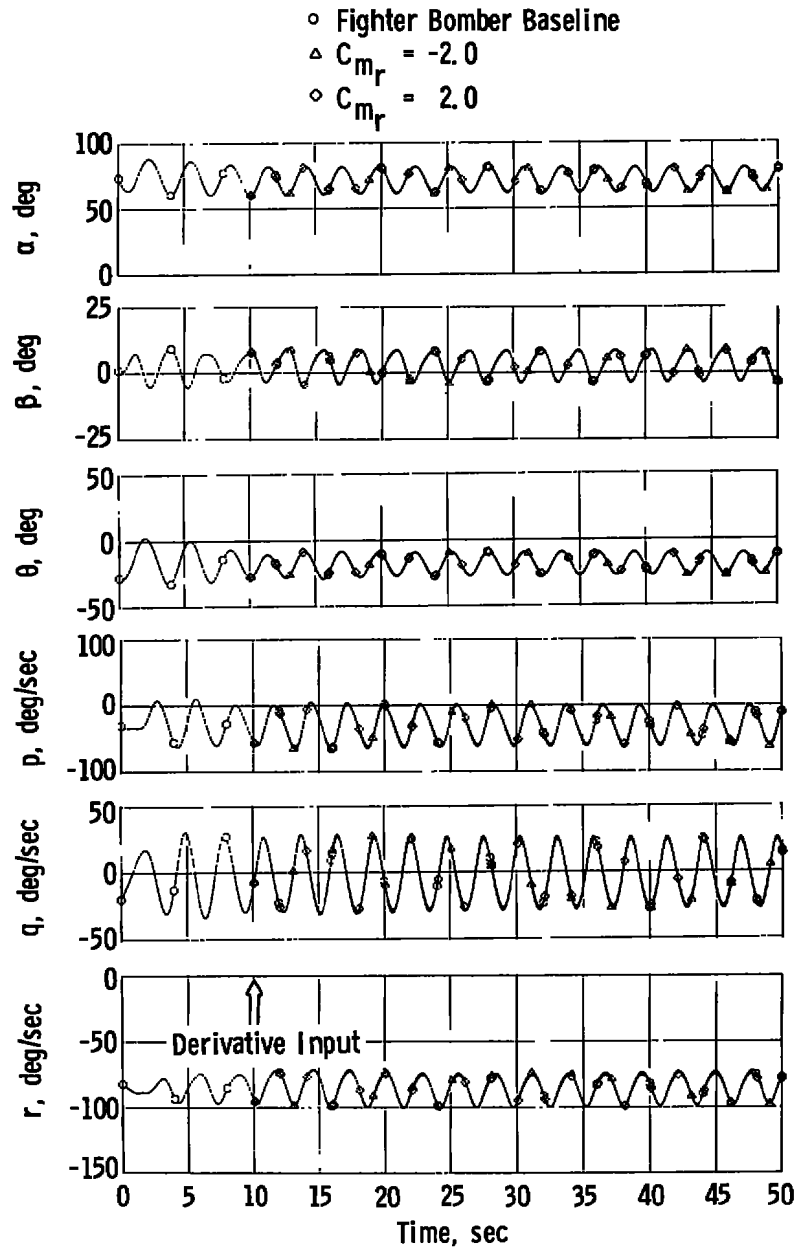


b. Fighter bomber-type aircraft
Figure 7. Concluded.

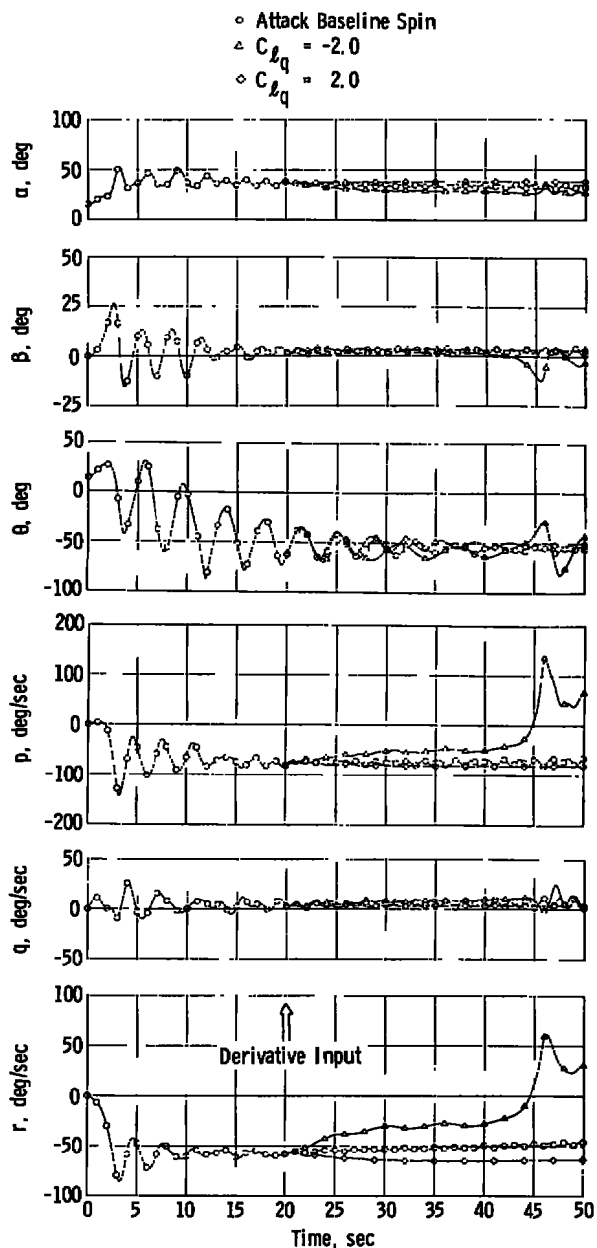


a. Attack-type aircraft

Figure 8. Spin sensitivity to C_{m_r} variation.

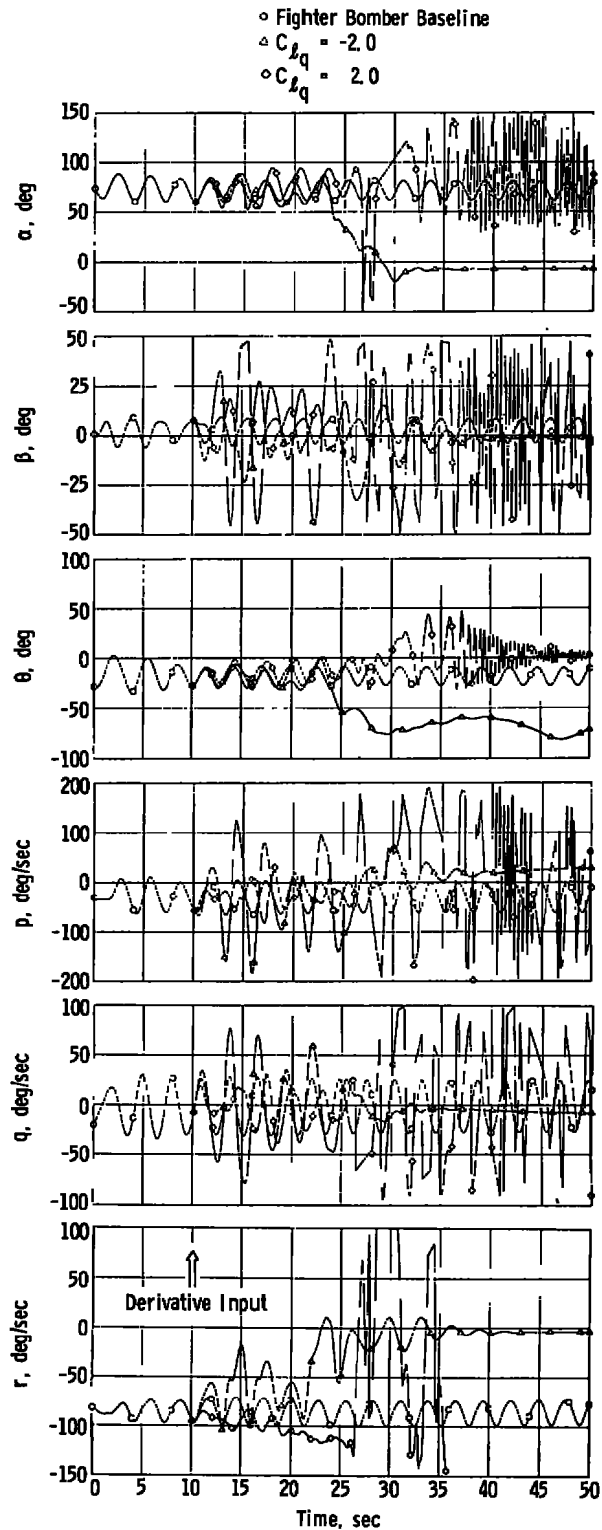


b. Fighter bomber-type aircraft
Figure 8. Concluded.

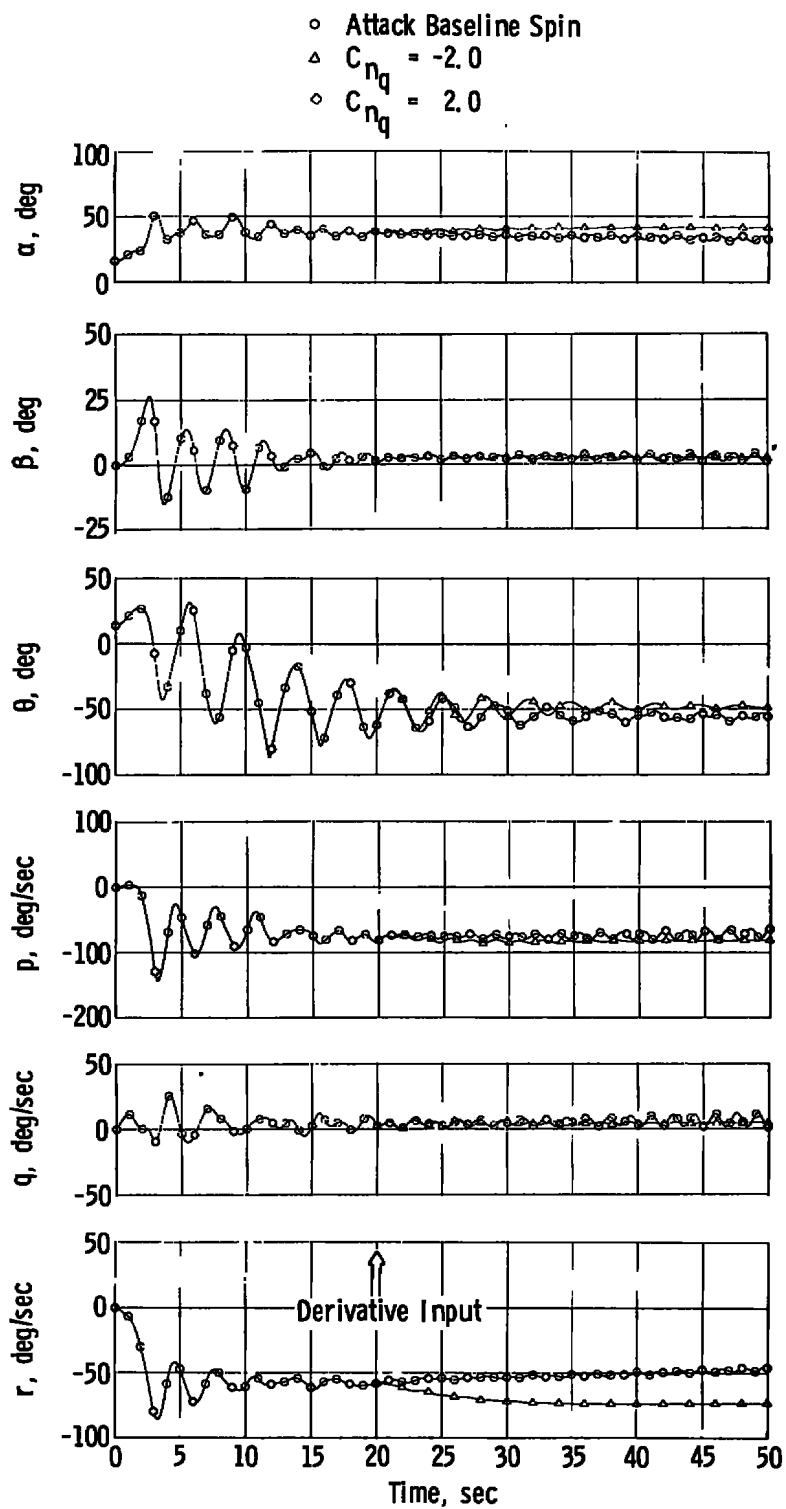


a. Attack-type aircraft

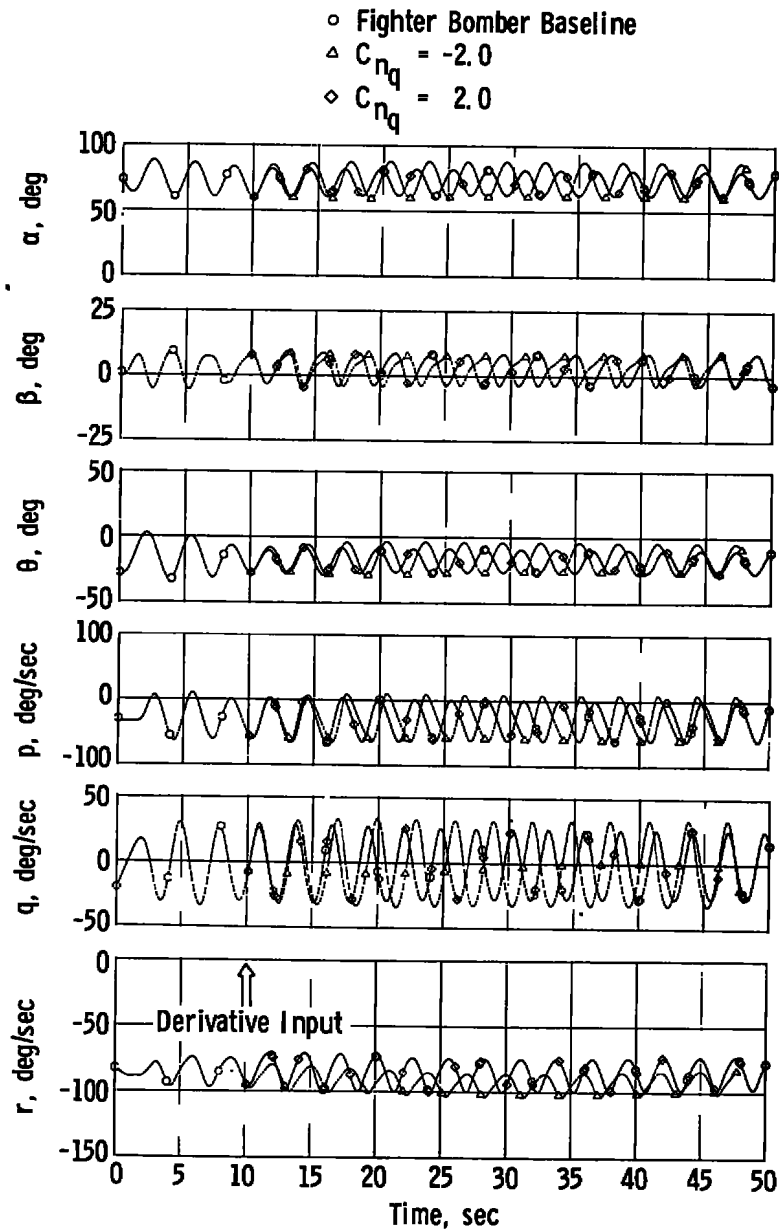
Figure 9. Spin sensitivity to C_{lq} variation.



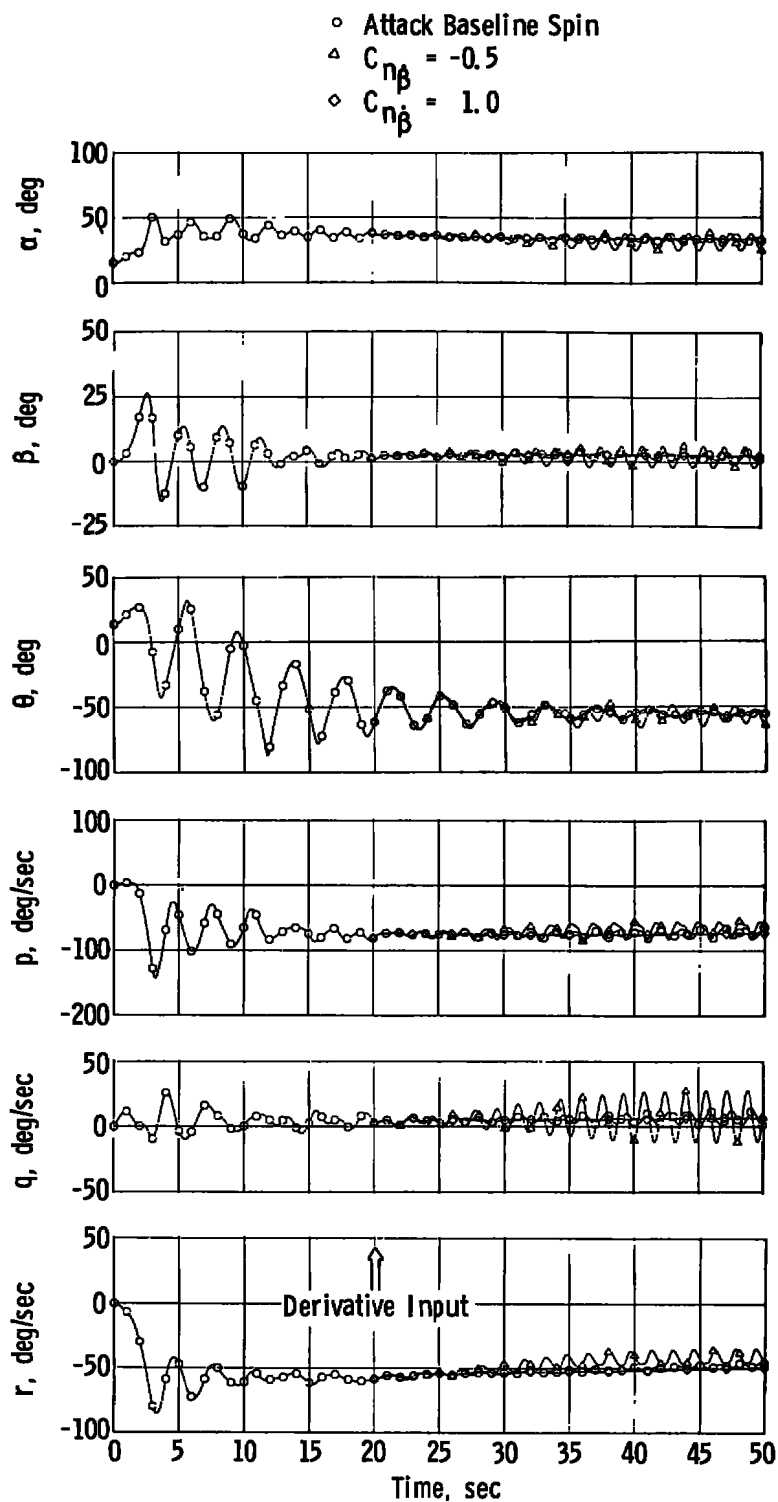
b. Fighter bomber-type aircraft
Figure 9. Concluded.



a. Attack-type aircraft
 Figure 10. Spin sensitivity to C_{nq} variation.

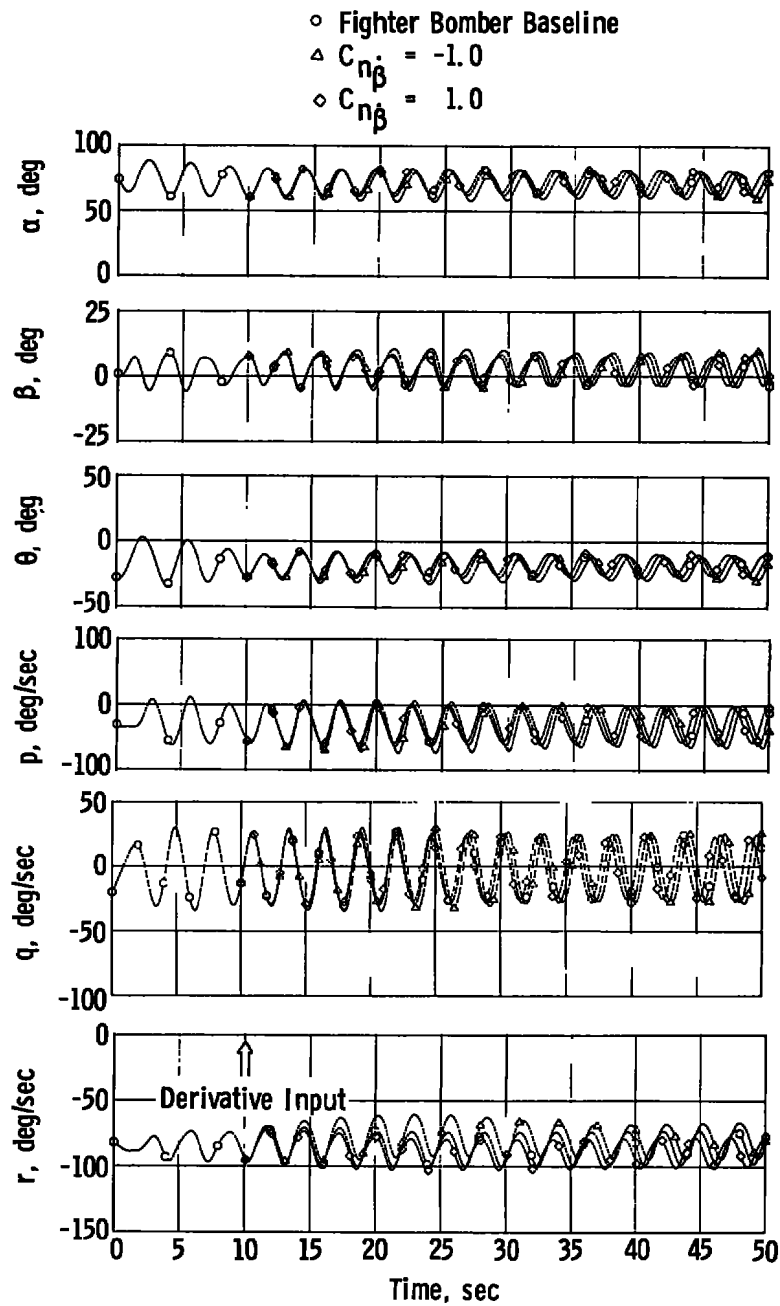


b. Fighter bomber-type aircraft
Figure 10. Concluded.

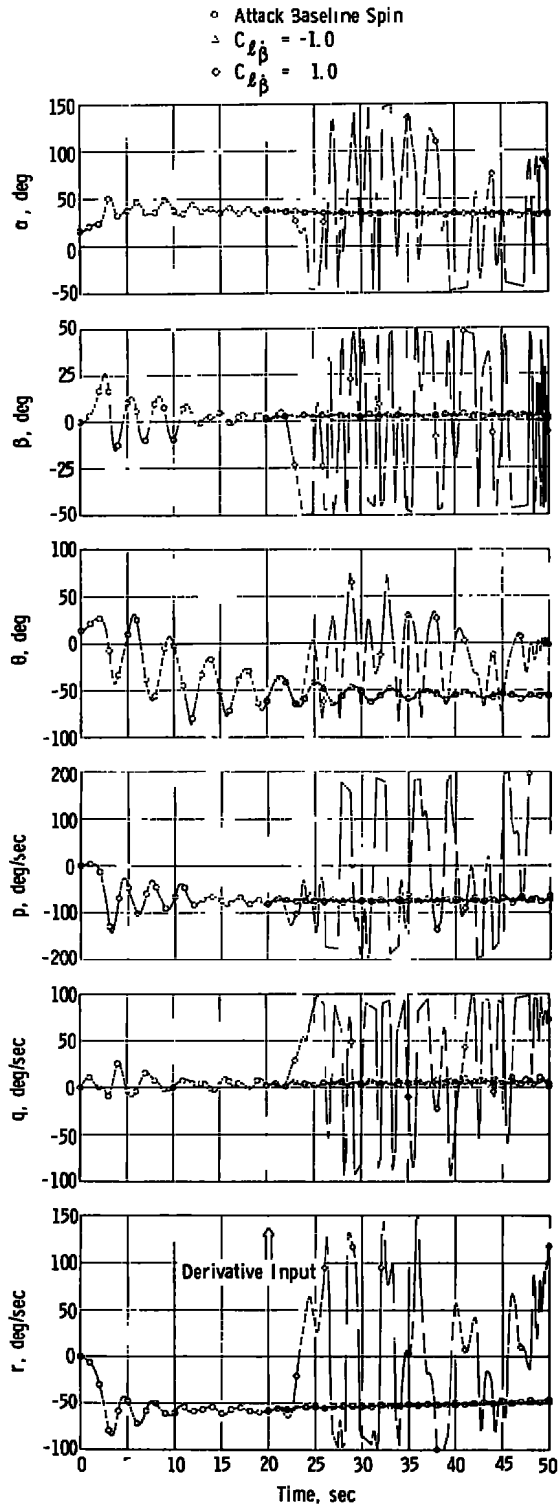


a. Attack-type aircraft

Figure 11. Spin sensitivity to $C_{n\beta}$ variation.

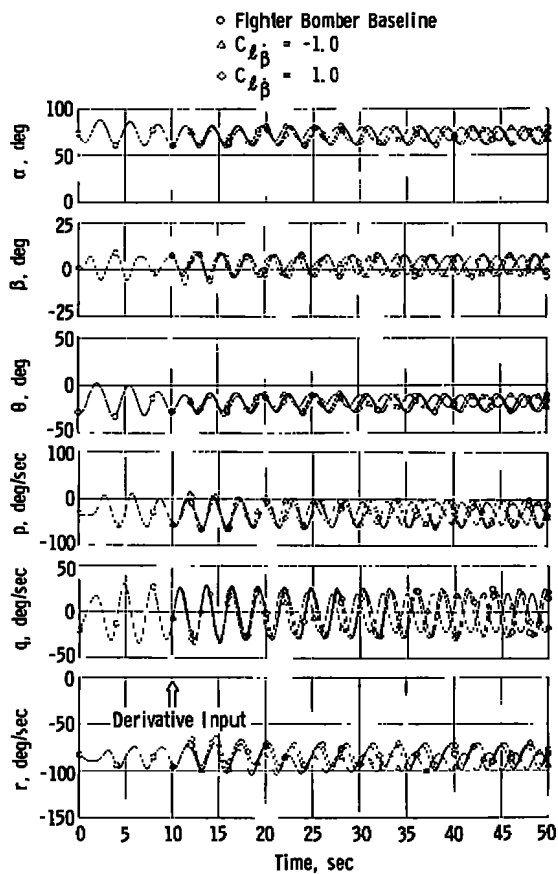


b. Fighter bomber-type aircraft
Figure 11. Concluded.

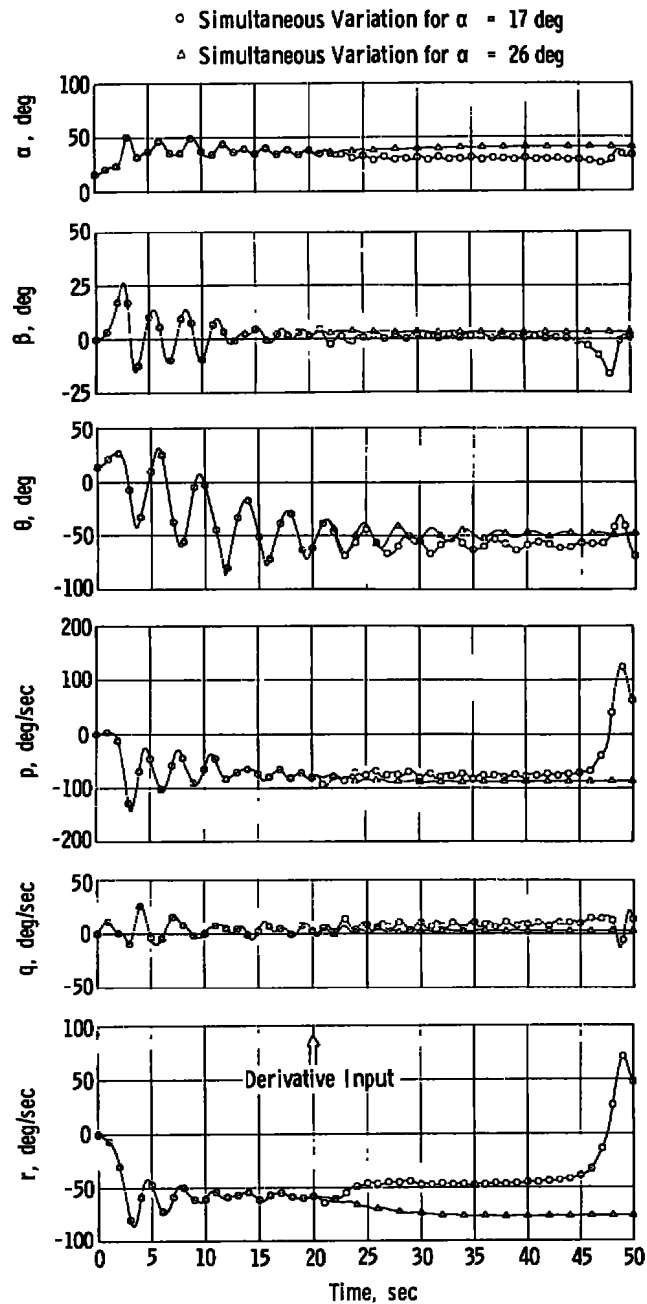


a. Attack-type aircraft

Figure 12. Spin sensitivity to $C_{L\dot{\beta}}$ variation.

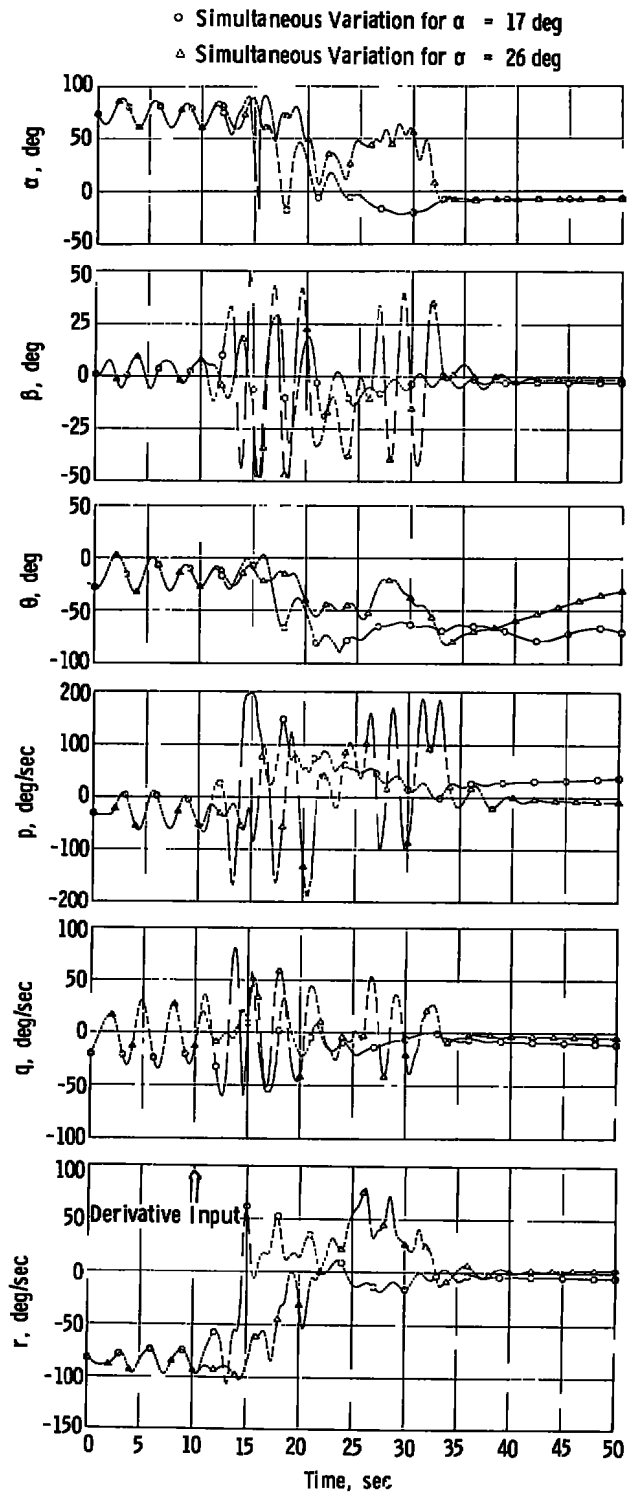


b. Fighter bomber-type aircraft
 Figure 12. Concluded.



a. Attack-type aircraft

Figure 13. Simultaneous derivative variation.



b. Fighter bomber-type aircraft
 Figure 13. Concluded.

Table 1. Aircraft Physical and Mass Characteristics

	<u>Attack-Type Aircraft</u>	<u>Fighter Bomber-Type Aircraft</u>
Mass	719 slugs	1147.5 slugs
I_X	15,927 slug-ft ²	22,600 slug-ft ²
I_Y	64,792 slug-ft ²	163,100 slug-ft ²
I_Z	75,976 slug-ft ²	182,000 slug-ft ²
I_{XZ}	3,885 slug-ft ²	5,450 slug-ft ²
S	375 ft ²	538.3 ft ²
b	38.73 ft	38.4 ft
c	10.84 ft	16.04 ft
cg	30 percent MAC	33.0 percent MAC

**Table 2. Cross-Coupling and Acceleration Derivatives
for Baseline Spin (Body Axis)**

$$\begin{aligned}
 C_{n\dot{\beta}} &= 0.25 \\
 C_{\ell\dot{\beta}} &= -0.35 \\
 C_{m\dot{r}} &= -0.75 \\
 C_{m\dot{p}} &= 0 \\
 C_{\lambda\dot{q}} &= 0 \\
 C_{n\dot{q}} &= 2.0
 \end{aligned}$$

Table 3. Dynamic Derivative Values for Individual Variations (Body Axis)

	<u>Max</u>	<u>Min</u>
$C_{n\dot{\beta}}$	1.0	-0.5
$C_{l\dot{\beta}}$	1.0	-1.0
C_{m_r}	2.0	-2.0
C_{m_p}	2.0	-2.0
$C_{l\dot{q}}$	2.0	-2.0
$C_{n\dot{q}}$	2.0	-2.0

Table 4. Dynamic Derivatives Used in Simultaneous Variations (Body Axis)

Case for Angle of Attack = 17 deg Case for Angle of Attack = 26 deg

$C_{n\dot{\beta}} = 0$	$C_{n\dot{\beta}} = 0.71$
$C_{l\dot{\beta}} = -0.5$	$C_{l\dot{\beta}} = -0.95$
$C_{m_r} = 0.4$	$C_{m_r} = -0.2$
$C_{m_p} = 0$	$C_{m_p} = 0$
$C_{l\dot{q}} = -2.0$	$C_{l\dot{q}} = 2.0$
$C_{n\dot{q}} = 0$	$C_{n\dot{q}} = 0.4$

APPENDIX A AERODYNAMIC MATHEMATICAL MODELS

a. Attack Aircraft Aerodynamic Mathematical Model (No Rotational Data)

$$F_X = q_\infty S [C_X(\alpha, \delta_H) + \Delta C_X(\delta_S, \alpha)]$$

$$F_Y = q_\infty S \left[C_Y(\alpha, \beta, \delta_H) + \Delta C_Y(\delta_A, \alpha) - \Delta C_Y(\delta_S, \alpha) + \Delta C_Y(\delta_R, \alpha) \right. \\ \left. + C_{Y_p}(\alpha) \frac{pb}{2v} + C_{Y_r}(\alpha) \frac{rb}{2v} \right]$$

$$F_Z = q_\infty S \left[C_Z(\alpha, \delta_H) - \Delta C_Z(\delta_A, \alpha) + \Delta C_Z(\delta_S, \alpha) + C_{Z_q}(\alpha) \frac{qc}{2v} + C_{Z_{\dot{\alpha}}}(\alpha) \frac{\dot{\alpha}c}{2v} \right]$$

$$M_X = q_\infty S b \left[C_\ell(\alpha, \beta, \delta_H) + \Delta C_\ell(\delta_A, \alpha) - \Delta C_\ell(\delta_S, \alpha) \right. \\ \left. + \Delta C_\ell(\delta_R, \alpha) + C_{\ell_r}(\alpha) \frac{rb}{2v} + C_{\ell_p}(\alpha) \frac{pb}{2v} + C_{\ell_q}(\alpha) \frac{qc}{2v} \right. \\ \left. + C_{\ell_{\dot{\beta}}} \frac{\dot{\beta}b}{2v} \right]$$

$$M_Y = q_\infty S c \left[C_m(\alpha, \delta_H) + \Delta C_m(\delta_A, \alpha) + \Delta C_m(\delta_S, \alpha) + \Delta C_{m_{\dot{\alpha}}}(\alpha, \delta_H) \frac{\dot{\alpha}c}{2v} \right. \\ \left. + C_{m_q}(\alpha, \delta_H) \frac{qc}{2v} + C_{m_p} \frac{pb}{2v} + C_{m_r} \left(\frac{rb}{2v} \right) \right]$$

$$M_Z = q_\infty S b \left[C_n(\alpha, \beta, \delta_H) + \Delta C_n(\delta_A, \alpha) - \Delta C_n(\delta_S, \alpha) - \Delta C_n(\delta_R, \alpha) \right. \\ \left. + C_{n_r}(\alpha) \frac{rb}{2v} - C_{n_p}(\alpha) \frac{pb}{2v} + C_{n_q} \frac{qc}{2v} + C_{n_{\dot{\beta}}} \frac{\dot{\beta}b}{2v} \right]$$

The data matrix was formulated as a function of the following variables and their associated ranges.

$$\alpha = 0 \text{ to } 90 \text{ deg}$$

$$\beta = -90 \text{ to } 90 \text{ deg}$$

$$\delta_H = -5 \text{ to } -25 \text{ deg}$$

$$\delta_A = -25 \text{ to } 25 \text{ deg}$$

$$\delta_R = -6 \text{ to } 6 \text{ deg}$$

$$\delta_S = 0 \text{ to } 60 \text{ deg}$$

**b. Fighter Bomber F-4 Aerodynamic Mathematical Model
(With Rotational Data)**

$$F_X = q_\infty S \left[C_X(\alpha, \beta, \delta_H) + \Delta C_X(\alpha, \beta, \delta_H, \Omega_{ss}) + C_{X_q}(\alpha) \frac{q_o c}{2v} \right]$$

$$F_Y = q_\infty S \left[C_Y(\alpha, \beta) + \Delta C_Y(\alpha, \beta, \delta_r) + \Delta C_Y(\alpha, \beta, \Omega_{ss}) \right. \\ \left. + C_{Y_p}(\alpha) \frac{p_o b}{2v} + C_{Y_r}(\alpha, \delta_H) \frac{r_o b}{2v} \right]$$

$$F_Z = q_\infty S \left[C_Z(\alpha, \beta, \delta_H) + \Delta C_Z(\alpha, \beta, \delta_H, \Omega_{ss}) + C_{Z_q}(\alpha) \frac{q_o c}{2v} \right]$$

$$M_X = q_\infty S b \left[C_\ell(\alpha, \beta) + \Delta C_\ell(\alpha, \beta, \delta_A) + \Delta C_\ell(\alpha, \beta, \delta_R) \right. \\ \left. + \Delta C_\ell(\alpha, \beta, \Omega_{ss}) + C_{\ell_p}(\alpha) \frac{p_o b}{2v} - C_{\ell_r}(\alpha, \delta_H) \frac{r_o b}{2v} \right. \\ \left. + C_{\ell_{\dot{\beta}}} \frac{\dot{\beta} b}{2v} + C_{\ell_q} \frac{q_o c}{2v} \right]$$

$$M_Y = q_\infty S c \left[C_m(\alpha, \beta, \delta_H) + \Delta C_m(\alpha, \beta, \delta_H, \Omega_{ss}) + C_{m_q}(\alpha) \frac{q_o c}{2v} \right. \\ \left. + C_{m_p} \left(\frac{p_o b}{2v} \right) + C_{m_r} \left(\frac{r_o b}{2v} \right) \right]$$

$$M_Z = q_\infty S b \left[C_n(\alpha, \beta) + \Delta C_n(\alpha, \beta, \delta_A) + \Delta C_n(\alpha, \beta, \delta_R) \right. \\ \left. + \Delta C_n(\alpha, \beta, \Omega_{ss}) + C_{n_p}(\alpha) \frac{p_o b}{2v} + C_{n_r}(\alpha, \delta_H) \frac{r_o b}{2v} \right. \\ \left. + C_{n_{\dot{\beta}}} \frac{\dot{\beta} b}{2v} - C_{n_q} \frac{q_o c}{2v} \right]$$

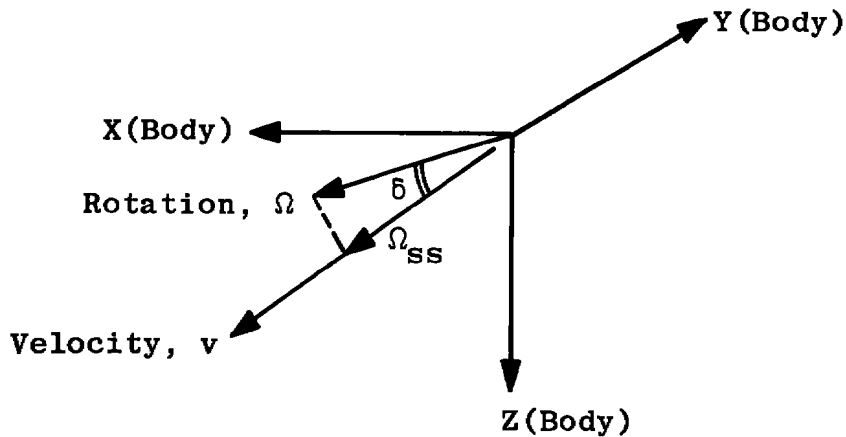
The data matrix was formulated as a function of the following variables and their associated ranges.

α	= 0 to 90	(Steady-State Data)
	55 to 90	(Rotational Data)
β	-40 to 40	(Steady-State Data)
	0 to 15	(Rotational Data)
δ_{II}	-21 to 7	
δ_A	-30 to 30	
δ_R	-30 to 30	
Ω_{ss}	-0.3 to 0.3	

APPENDIX B

ROTATIONAL BALANCE DATA IMPLEMENTATION

The rotational balance data incorporated in the aerodynamic data matrices of Appendix A were obtained with a model/balance rotating in the wind tunnel with its rotational vector aligned with the velocity vector of the wind tunnel. Because the rotational and velocity vectors are normally misaligned in spinning flight, the direct implementation of the rotational-balance data as a function of the total rotational rate vector (Ω) is in error. The method used for implementing the data resolves a component (Ω_{ss}) of the total rotational vector along the aircraft velocity vector. This component rotational vector (Ω_{ss}) may now be used in determining the incremental coefficients to be included in the aerodynamic data matrices. The determination of the magnitude of the steady-state rotational vector (Ω_{ss}) and its inclination (δ) to the aircraft total rotational vector (Ω) is the same as that used in Ref. 7 and is outlined below.



$$\bar{v} = v\bar{i} + v\bar{j} + w\bar{k}$$

Total Velocity Vector

$$\bar{r} = p\bar{i} + q\bar{j} + r\bar{k}$$

Total Rotational Vector

$$\bar{\Omega}_{ss} = p_{ss}\bar{i} + q_{ss}\bar{j} + r_{ss}\bar{k}$$

Steady-State Rotational Vector along Velocity Vector \bar{v}

$$|\Omega_{ss}| = |\Omega| \cos \delta$$

$$\bar{\Omega} \cdot \bar{v} = |\Omega| |\bar{v}| \cos \delta$$

$$up + vq + wr = |\Omega| |\bar{v}| \cos \delta$$

Substituting:

$$|\Omega_{ss}| = \frac{up + vq + wr}{|\bar{v}|}$$

Knowing the magnitude and direction of the steady-state rotational vector, its components may be resolved into body-axis components.

$$p_{ss} = \Omega_{ss} \cos \beta \cos \alpha$$

$$q_{ss} = \Omega_{ss} \sin \beta$$

$$r_{ss} = \Omega_{ss} \cos \beta \sin \alpha$$

These body-axis components of the steady-state rotation are now used for determining the magnitude of the oscillatory rate components.

$$p_o = p - p_{ss}$$

$$q_p = q - q_{ss}$$

$$r_o = r - r_{ss}$$

The oscillatory components are used in conjunction with the dynamic oscillatory derivatives in the aerodynamic data matrices. Utilizing the rotational and oscillatory derivatives in the manner outlined accounts for oscillations that normally occur in addition to an aircraft steady-state spinning motion.

In the subject investigation, the rotational-balance data were applied when the misalignment angle (δ) between the rotational vector (Ω) and velocity vector (v) was less than 40 deg. Above 40 deg, the rotational-balance increments to the aircraft aerodynamic matrix were zeroed with an exponential decay function. Under these conditions, the oscillatory rates (p_o , q_o , r_o) become equal to the total rotational rates (p , q , r). Likewise, when the total rotational vector is aligned with the velocity vector, the case where $\delta = 0$, the aircraft is in a flat spin and the oscillatory rate components are zero.

NOMENCLATURE

b	Wing span, ft
c	Wing chord, ft
F_X, F_Y, F_Z	Forces along the aircraft body reference axis in the X, Y, and Z directions, lb
g	Acceleration caused by gravity, ft/sec ²
I_X, I_Y, I_Z	Moments of inertia, body axis, slug-ft ²
I_{XZ}	Product of inertia, body axis, slug-ft ²
M_X, M_Y, M_Z	Moments about the aircraft X, Y, and Z body reference axes, ft-lb
M_{YT}	Moment contribution from engine thrust about the aircraft Y body axis, ft-lb
M_{YG}, M_{ZG}	Engine gyroscopic moments about aircraft Y and Z body axes, ft-lb
m	Aircraft mass, slug
p, q, r	Total roll, pitch, and yaw rates about aircraft X, Y, and Z body axes, rad/sec, deg/sec
p_o, q_o, r_o	Oscillatory roll, pitch, and yaw rates about aircraft X, Y, and Z body axes, rad/sec, deg/sec
p_{ss}, q_{ss}, r_{ss}	Steady-state roll, pitch, and yaw rates about aircraft X, Y, and Z body axes, rad/sec, deg/sec
$\dot{p}, \dot{q}, \dot{r}$	Total roll, pitch, and yaw accelerations about aircraft X, Y, and Z body axes, rad/sec ² deg/sec
q_∞	Dynamic pressure, lb/ft ²
S	Wing area, ft ²
T_X, T_Z	Aircraft thrust components along aircraft X and Z body axes, lb
u, v, w	Velocity components along aircraft X, Y, and Z body axes, ft/sec

u,v,w	Acceleration components along aircraft X, Y, and Z body axes, ft/sec ²
V_{∞}	Free-stream velocity, ft/sec
X,Y,Z	Orthogonal body-axis system fixed in the aircraft with the X-axis along the longitudinal centerline of the body, the Y-axis normal to the plane of symmetry, and the Z-axis in the plane of symmetry
α	Aircraft angle of attack, deg
$\dot{\alpha}$	Rate of change of angle of attack, deg/sec
β	Aircraft angle of sideslip, deg
$\dot{\beta}$	Rate of change of angle of sideslip, deg/sec
δ_A	Aircraft aileron deflection, positive deflection produces a negative moment, deg
δ_H	Aircraft horizontal stabilizer deflection, trailing edge down, positive, deg
δ_R	Aircraft rudder deflection, trailing edge left, positive, deg
δ_S	Aircraft spoiler deflection, deg
θ	Aircraft angle of pitch, deg
ϕ	Aircraft angle of roll, deg
Ω	Aircraft total spin rate, rad/sec
Ω_{ss}	Aircraft steady-state spin rate, rad/sec

STATIC AERODYNAMIC COEFFICIENTS: BODY AXIS

$$C_X = F_X/q_{\infty} S$$

$$C_{\ell} = M_X/q_{\infty} S b$$

$$C_Y = F_Y/q_{\infty} S$$

$$C_m = M_Y/q_{\infty} S c$$

$$C_Z = F_Z/q_{\infty} S$$

$$C_n = M_Z/q_{\infty} S b$$

DYNAMIC STABILITY DERIVATIVES: BODY AXIS

$$C_{Y_p} = \partial C_Y / \partial (pb/2V_\infty)$$

$$C_{\ell_r} = \partial C / \partial (rb/2V_\infty)$$

$$C_{m_r} = \partial C_m / \partial (rb/2V_\infty)$$

$$C_{Y_r} = \partial C_Y / \partial (rb/2V_\infty)$$

$$C_{\ell_{\dot{\beta}}} = \partial C / \partial (\dot{\beta}b/2V_\infty)$$

$$C_{m_{\dot{\alpha}}} = \partial C_m / \partial (\dot{\alpha}c/2V_\infty)$$

$$C_{\ell_p} = \partial C_{\ell} / \partial (pb/2V_\infty)$$

$$C_{m_p} = \partial C_m / \partial (pb/2V_\infty)$$

$$C_{n_p} = \partial C_n / \partial (pb/2V_\infty)$$

$$C_{\ell_q} = \partial C_{\ell} / \partial (qc/2V_\infty)$$

$$C_{m_q} = \partial C_m / \partial (qc/2V_\infty)$$

$$C_{n_q} = \partial C_n / \partial (qc/2V_\infty)$$

$$C_{n_r} = \partial C_n / \partial (rb/2V_\infty)$$

$$C_{X_q} = C_X / \partial (qc/2V_\infty)$$

$$C_{n_{\dot{\beta}}} = \partial C_n / \partial (\dot{\beta}b/2V_\infty)$$

$$C_{Z_q} = \partial C_Z / \partial (qc/2V_\infty)$$